doi: 10.22564/rbgf.v9i2.1113

GLOBAL COMPILATION OF PHASE AND GROUP VELOCITIES OF FUNDAMENTAL MODE RAYLEIGH WAVES IN THE PERIOD RANGE 20 TO 100 SEC

João Willy Correa Rosa[1*] & Keiiti Aki[2]

We collected a large amount of phase velocity data for fundamental mode Rayleigh waves with period ranging between 20 and 100 seconds from the literature. These data were classified and organized in a way that can now be used by other authors. These data were used to determine the average phase velocity for three regionalized and widely used Earth models. These values served as an initial model used in the unwrapping process of the phase spectra measured in the second part of our study, where we studied the records of Rayleigh waves generated by a set of 45 earthquakes, which had their source mechanism and focal depth determined by other authors. The data from this second part of the study complement the data collected from the existing literature. We have then obtained an increased (we had more than doubled the initial amount of data available) data set which also includes the group velocity data from the second part of our study. This increased data set is organized to facilitate future studies on wave propagation, source mechanics and Earth structure.

COMPILAÇÃO GLOBAL DAS VELOCIDADES DE FASE E DE GRUPO NO MODO FUNDAMENTAL DE ONDAS DE RAYLEIGH COM PERÍODO VARIANDO NO INTERVALO ENTRE 20 E 100 SEG – Neste estudo, mostramos uma grande quantidade de dados de velocidade de fase de ondas Rayleigh no modo fundamental, com valores de período variando entre 20 e 100 segundos, que foram compilados da literatura geofísica internacional. Estes dados foram classificados e organizados de modo que possam ser agora utilizados de modo rotineiro por pesquisadores em sismologia. Neste trabalho, os dados em questão foram empregados para determinação da velocidade de fase média em três modelos globais de regionalização dos tipos tectônicos encontrados na Terra. Os valores determinados serviram, na segunda parte deste estudo, para definir um modelo inicial, usado no processo de desdobramento do espectro de fase de ondas geradas por um conjunto de 45 sismos, cujo mecanismo focal e profundidade focal foram determinados por outros autores em estudos prévios. Os dados de velocidade de fase determinados nesta segunda parte do trabalho foram então acrescentados, para efeito de complementação, aos dados compilados e organizados na primeira etapa. Assim, obtivemos um banco de dados consideravelmente mais extenso que o primeiro (o resultado de nossas medidas praticamente dobrou a quantidade inicial de dados disponíveis na literatura), que pode agora ser empregado em estudos futuros sobre propagação de ondas, mecanismo focal e sobre estrutura interna terrestre. Além das novas medidas de velocidade de fase mostradas aqui, nosso novo banco de dados inclui ainda um grande conjunto inédito de medidas de velocidade de grupo destas ondas, correspondente aos percursos estudados na segunda etapa.

1. Department of Earth, Atmospheric and Planetary Sciences, Massachusetts Institute of Technology, Cambridge, MA 02139, USA
2. Department of Geological Sciences, University of Southern California, Los Angeles, CA 90089-0740, USA
* Present address: Instituto de Geociências, Departamento de Geologia Geral e Aplicada, Universidade de Brasília, 70910 Brasília, DF

INTRODUCTION

The objective of this work is to compile all phase velocity data available in the literature for fundamental mode Rayleigh waves in the 20 to 100 seconds period range, and to measure phase velocities for additional paths covering regions that were not included in previous studies, so that a larger, and more complete, data set is readily available for the seismological community.

Previous studies on regionalization of phase velocity of fundamental mode Rayleigh waves were restricted to parts of the Earth in the period range considered here. The global information on phase velocity of shorter period surface waves is essential for the application of the moment tensor inversion technique to surface waves from smaller earthquakes which do not generate sufficient long-period energy. It is also useful for more detailed studies of the structure of lithosphere and asthenosphere.

In order to gather this data set we have divided this work into two parts.

To pursue our objective of global coverage, we started this project by collecting the phase velocity data already measured by other authors. We used published phase velocity dispersion curves measured using the one-, two-, or, in some cases, three-station method, and formed a complete collection of existing data.

We constructed initial models of global phase velocity distribution using the data collected from the literature by grouping the data according to the tectonic types of their paths. Similar studies on a global scale for this period range have been done previously by a number of authors including Oliver (1962), Brune (1969), Dorman (1969), Knopoff (1972, 1983) and Sobel & Seggern (1978). We adopted three different Earth models due to Okal (1977), Leveque (1980) and Jordan (1981). These models have been used in the study of waves with longer period: Silver & Jordan (1981) used the model of Jordan (1981), Dziewonski & Steim (1982) used a four-region model very similar to that introduced by Leveque (1980), while Nataf et al. (1986) considered the model of Okal (1977). We also used a statistical test to verify the effectiveness of these models for grouping the data set.

In the second part of our work, we more than doubled the number of paths for which the phase velocity had been determined before. We achieved this by measuring phase velocity between the epicenter and WWSSN stations for 45 earthquakes, for which focal mechanisms have been determined by other authors using body waveform data. We also processed a large amount of group velocity measurements, to establish a similar set of globally regionalized group velocity models.

EXISTING PHASE VELOCITY DATA FOR FUNDAMENTAL MODE RAYLEIGH WAVES IN THE 20 TO 100 SEC PERIOD RANGE

We will first review the evolution of the studies on phase velocity of surface waves. In this case, each of the methods used for such measurements will be considered. A complete review of each of the studies, summarizing the main constraints used in the measurements, as well as the error estimates made by each author, can be found in the work of Rosa (1986).

The three-station methods

The first phase velocity measurement of Rayleigh waves was done by Press (1956a, b) using a three-station array. This method is widely known as the three-station (or tripartite) method. In his work, he established a sequence of phase velocity data interpretation that is still followed in recent papers: measurement of phase velocity, calculation of theoretical phase velocity curves for a given structure, comparison of observed and theoretical curves, and interpretation of the structure which theoretical dispersion curve had the best fit under the light of additional geological and geophysical information available for the area.

Press (1956a, b) identified the crests and troughs of Rayleigh waves generated by an event at three stations located in southern California, and measured the difference in travel time observed among stations. From these differential travel times, the velocity and the angle of incidence of the wave are calculated assuming that incident wave is a plane wave.

We present a simple sketch of the three-station method of Press (1956a, b) in Fig. 1, where a surface wave with period T, and phase velocity c(T) approaches an array composed of stations 1, 2 and 3. The phase velocity measured by the observation of the wave from arrival at each station can be obtained from

$$c(T) = \frac{\Delta_{12} \sin A(T)}{\Delta t_{12}(T)} = \frac{\Delta_{13} \sin [A(T) + \alpha]}{\Delta t_{13}(T)} \qquad (1)$$

where

Δ_{12} and Δ_{13}, $\Delta t_{12}(T)$ and $\Delta t_{13}(T)$ are the distance between station pairs 1-2 and 1-3, and the arrival time differences of the phase with period T at these stations pairs, respectively.

α is the angle between the triangle legs containing the station pairs 1-2 and 1-3.

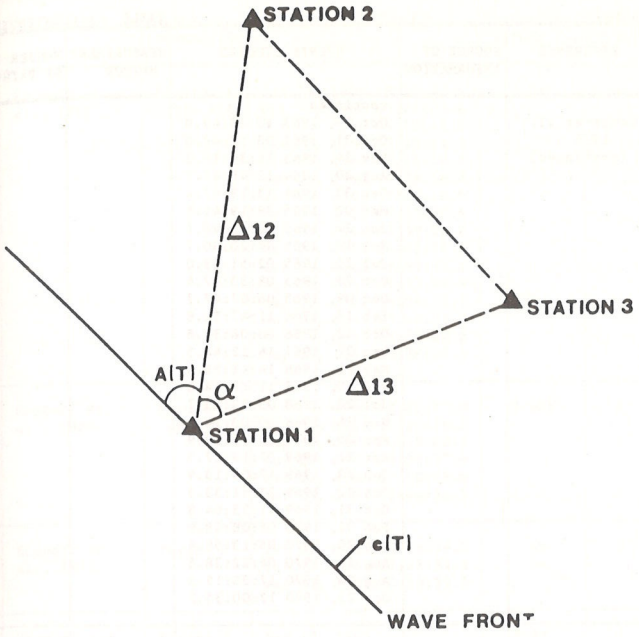

Figure 1. Schematic representation of plane wave incident on a tripartite array, where observed arrival times are used to determine the phase velocity c(T) for the region covered by the triangle, and the incident angle A(T).

Figura 1. Representação esquemática do plano de onda incidente em um arranjo de três estações, onde as observações de tempo de chegada das ondas são usadas para determinação da velocidade de fase média, c(T), para a região envolvida pelo triângulo formado pelas três estações. Neste caso, também é determinado o ângulo de incidência das ondas, A(T).

A(T) is the incident angle of the wave front. It can be measured using Snell's law,

$$A(T) = \tan^{-1}\left[\frac{\sin\alpha}{[\Delta t_{12}(T)\,\Delta_{13}]/[\Delta t_{13}(T)\,\Delta_{12}] - \cos\alpha}\right] \qquad (2)$$

Ewing & Press (1959) chose an event that occurred in the Samoa Islands as the source for a study of the distribution of Rayleigh waves phase velocity in the whole United States. This was the first attempt to regionalize the phase velocity values of fundamental mode Rayleigh waves.

Knopoff et al. (1966) used events located near a great circle connecting two of the stations of the tripartite array. They found that the third station from the array has little influence on the calculated three-station phase velocity, so that we can assign the measured velocity value to the path between the two stations. We included the results obtained by this technique in Tab. 1, where we collected all the phase velocity data associated with particular paths.

TABLE 1

REFERENCE	SOURCE OF INFORMATION	EVENTS STUDIED	MEASUREMENT METHOD	NUMBER OF PATHS
Bache et al., 1978	Figure 2	Apr 14, 1966 14:13:43 Jun 02, 1966 15:30:00 Jun 06, 1966 14:00:00	1 SM	6
Baldi et al, 1979 (some paths are also in Baldi et al, 1978)	Figure 1	Mar 25, 1972 22:59:40.3 Mar 31, 1972 15:36:53.5 Feb 19, 1973 08:42:52.1 Mar 12, 1973 19:39:21.0 Nov 11, 1973 02:43:06.2 Jan 08, 1974 21:47:21.6 Jan 22, 1974 13:28:20.0 Jun 24, 1974 20:34:35.4 May 25, 1975 19:04:34.4 Jan 23, 1976 15:14:16.0	2 SM	8
Berry and Knopoff, 1967	Figure 3	Jun 11, 1961 05:10:26.3 Jul 28, 1961 01:05:30.0 Aug 08, 1961 12:18:23.1 Aug 17, 1961 21:16:30.1 Aug 27, 1961 01:50:51.8 Aug 30, 1961 03:35:02.7	3 SM†	7
Biswas, 1971	Tables V and VI	Sep 16, 1964 22:23:36.3 Sep 17, 1964 15:02:00.9 Sep 19, 1964 05:08:15.1 Oct 12, 1964 21:55:33.2 Nov 30, 1964 12:27:38.6 Jun 02, 1965 23:40:23.5 Jul 05, 1965 08:31:58.3 Aug 20, 1965 21:21:51.5 Nov 15, 1965 11:18:50.3 Nov 16, 1965 15:24:43.0 Sep 02, 1966 07:59:05.2	2 SM	18
Bloch and Hales, 1968	Figure 7	Mar 01, 1963 19:14:11.1 Mar 24, 1963 02:07:09.4 Mar 25, 1963 22:46:16.7 Nov 24, 1964 12:40:51.4 Nov 30, 1964 12:27:38.6 May 29, 1965 15:36:31.9 Sep 19, 1965 13:55:39.9 Dec 19, 1965 22:06:32.7	2 SM	8
Bolt and Niazi, 1964	Table 3	Feb 01, 1956 01:32:56.9 Jun 29, 1959 07:16:06.0	2 SM	2
Brooks, 1969	Figure 4 Table 5	Jan 23, 1965 16:09:01.9 Feb 13, 1966 06:35:55.7 Mar 02, 1966 07:32:42.6 May 25, 1966 08:28:58.6 Aug 10, 1966 12:33:42.2 Sep 07, 1966 05:53:45.7	2 SM 1 SM	3 6
Brune et al., 1960	Figures 6 and 11	Oct 18, 1958 15:00:00 Oct 22, 1958 08:21:11	1 SM	2
Brune and Dorman, 1963	Tables 3 and 4	Jan 07, 1956 16:41:04 Jun 03, 1956 05:19:23 Sep 14, 1958 14:21:37 Nov 12, 1958 06:09:10 Jan 30, 1959 05:17:32 Jun 14, 1959 00:11:57 Jul 09, 1959 16:05:18 Nov 03, 1959 09:40:05	2 SM 1 SM	9 5
Burkhard, 1977	Table 1	Mar 07, 1963 05:21:56.6 Mar 29, 1965 10:47:37.6 Jul 29, 1965 08:29:21.2 Aug 20, 1965 21:21:49.7 Oct 01, 1965 08:52:04.4 Nov 12, 1965 17:52:27.6 Dec 06, 1965 11:34:48.9 Feb 10, 1966 14:21:11.2 Jun 28, 1966 04:26:13.4 Jul 04, 1966 18:33:37.1 Aug 07, 1966 02:13:04.7 Aug 07, 1966 17:36:27.3 Sep 09, 1966 10:02:25.1 Jan 19, 1967 12:40:09.5 Apr 09, 1968 02:28:59.1	1 SM	37
Calcagnile and Panza, 1978	Table II	Dec 28, 1967 06:26:15.8 Aug 05, 1968 16:17:04.8 Sep 17, 1969 18:40:45.8	2 SM	3

TABLE 1 (CONTINUED)

REFERENCE	SOURCE OF INFORMATION	EVENTS STUDIED	MEASUREMENT METHOD	NUMBER OF PATHS
Calcagnile and Panza, 1979	Table 2	Apr 04, 1975 05:16:16.2	N SM	1
Calcagnile and Panza, 1980	Table 1	Mar 11, 1965 17:07:05.5 Feb 23, 1976 15:14:16.0	2 SM	2
Calcagnile et al., 1984	Table 2	May 19, 1963 01:03:06.2 Jul 14, 1963 05:41:43.0 Jan 27, 1964 01:12:23.5 Mar 19, 1964 09:42:34.9	2 SM	4
Caputo et al., 1976	Table I	Apr 03, 1972 18:52:59.3 Apr 03, 1972 20:36:22.2	2 SM	2
Chang, 1979	Table 4	Aug 25, 1964 13:47:20.6 Dec 26, 1964 14:30:29.1 Feb 13, 1966 10:44:41.3 Mar 07, 1966 21:29:17.4 Apr 25, 1966 23:22:49.3 Jun 06, 1966 07:46:16.1 Mar 31, 1969 07:15:54.4 Oct 14, 1970 07:29:58.6 Dec 28, 1974 12:11:43.7	1 SM	40
Chandhury, 1966	Figure 6	Jun 19, 1963 10:47:24.7 Jun 21, 1963 15:26:31.0 Jan 22, 1964 15:58:46.5 Feb 27, 1964 15:10:48.8 Feb 28, 1964 17:47:05.9	1 SM	5
Forsyth, 1973	Table 4	Mar 07, 1963 05:21:59.6 Apr 19, 1964 05:13:00.5 Oct 06, 1964 07:17:56.7 Oct 12, 1964 21:55:34.0 Nov 03, 1965 18:21:08.6 Nov 06, 1965 09:21:48.6 Nov 25, 1965 10:50:40.2 Jul 20, 1966 13:22:53.6 Dec 29, 1966 11:56:23.1 Jan 21, 1967 02:54:00.4	1 SM 2 SM	76 2
		Apr 01, 1967 10:41:00.2 Jun 26, 1969 02:30:58.4 Sep 09, 1969 15:23:10.8 Sep 20, 1969 15:26:41.5 Nov 18, 1970 20:10:58.2 May 09, 1971 08:25:01.7		
Forsyth, 1985	Table	Feb 07, 1965 Oct 01, 1965 May 15, 1966 Mar 19, 1967	1 SM	23
Fouda, 1973	Tables 5 thru 9	Oct 11, 1964 21:15:03.9 Nov 30, 1964 12:27:38.6 Apr 29, 1965 15:28:43.4 Aug 18, 1966 10:33:16.5 Feb 02, 1967 06:25:49.5	2 SM	7
Gabriel and Kuo, 1966	Figures 3 and 4	Nov 03, 1963 03:10:12.7 Nov 23, 1963 07:50:46.3 Dec 16, 1963 01:51:30.6 Feb 10, 1964 17:27:58.0 Feb 29, 1964 23:49:40.8 Jul 05, 1964 19:07:57.8 Jul 08, 1964 11:55:39.0	2 SM	1
Goncz et al., 1975	Figure 5	Dec 25, 1962 12:09:45.6 Mar 28, 1963 11:12:31.3 Mar 28, 1963 23:29:14.6 Mar 31, 1963 19:22:53.3 Apr 02, 1963 04:43:30.9 May 13, 1963 22:48:10.3 May 18, 1963 12:20:31.9 Jun 02, 1963 10:00:00.1 Jun 15, 1963 15:30:37.7 Jun 17, 1963 18:30:54.3 Jun 24, 1963 16:17:15.4 Jul 14, 1963 00:02:22.8 Aug 13, 1963 21:52:37.4 Aug 14, 1963 02:46:44.1 Oct 02, 1963 03:31:27.0 Oct 04, 1963 02:47:32.1 to be continued	2 SM	9

TABLE 1 (CONTINUED)

REFERENCE	SOURCE OF INFORMATION	EVENTS STUDIED	MEASUREMENT METHOD	NUMBER OF PATHS
Goncz et al., 1975 (continued)		continued Oct 27, 1963 10:38:49.0 Oct 31, 1963 03:17:42.0 Nov 24, 1963 16:30:16.0 Aug 20, 1964 12:48:47.7 Dec 30, 1964 13:19:47.4 Mar 02, 1965 09:19:41.6 Jun 27, 1965 09:45:48.7 Jul 17, 1965 07:20:30.7 Jul 21, 1965 02:51:39.0 Oct 23, 1965 08:33:47.4 Dec 09, 1965 06:07:47.7 Feb 17, 1966 11:47:56.8 Oct 12, 1966 00:06:38.8 Dec 27, 1967 16:22:48.5 May 26, 1968 14:41:52.0 Jul 10, 1968 11:16:44.6 Jul 22, 1968 05:09:15.7 Nov 26, 1968 00:03:14.3 Apr 05, 1969 02:18:29.9 Apr 21, 1969 07:19:27.5 Jun 29, 1969 17:09:13.9 Oct 22, 1969 22:51:33.5 Oct 31, 1969 11:33:04.8 Feb 04, 1970 05:08:48.0 Jun 25, 1970 05:13:58.6 Aug 13, 1970 04:22:38.5 Aug 24, 1970 12:30:19.5 Oct 25, 1970 12:00:35.2		
Gregersen, 1970	Figure 3	Apr 02, 1964 01:11:43.5 Apr 03, 1964 04:12:39.4 Jun 14, 1964 12:15:31.3 Jun 30, 1964 13:46:18.5 Jul 05, 1964 19:07:57.8 Jul 25, 1964 19:31:07.0 Jul 28, 1964 21:38:43.5 Oct 21, 1964 07:38:31.0 Jan 12, 1965 13:32:24.0 Feb 26, 1965 08:55:42.2 Mar 09, 1965 17:57:53.7 Mar 13, 1965 04:08:40.5 Mar 22, 1965 22:56:26.5 Mar 28, 1965 16:33:14.6 Apr 05, 1965 03:12:54.2 Apr 09, 1965 23:57:03.2	2 SM	2
		Apr 29, 1965 15:28:43.3 May 19, 1965 06:03:58.9 Jun 21, 1965 00:21:14.5 Sep 09, 1965 10:02:25.4 Nov 13, 1965 04:33:53.0 Dec 06, 1965 11:34:53.7 Dec 15, 1965 23:05:20.7 Jan 23, 1966 01:56:38.0 Mar 07, 1966 01:16:05.8 Mar 27, 1966 18:53:41.3 May 09, 1966 00:42:55.6 Jul 12, 1966 18:53:08.5 Jul 27, 1966 04:48:59.4 Aug 19, 1966 12:22:09.6 Jan 20, 1967 01:57:23.1		
Gumper and Pomeroy, 1970	Figures 3 thru 7	Jan 05, 1964 23:46:10.7 Aug 25, 1964 13:47:20.6 Jul 12, 1966 18:53:10.4	2 SM	8
Gupta et al., 1977	Figure 4	Jul 09, 1964 16:39:49	2 SM	1
James, 1971	Figures 6, 8,9,10,11, 12,13,17	Feb 21, 1966 00:22:29.5 Mar 20, 1966 01:42:49.9 Sep 14, 1966 23:18:40.8 Sep 15, 1966 11:51:56.4 Oct 11, 1966 16:25:55.1 Apr 19, 1968 09:04:27.3 Dec 05, 1968 09:44:11.0 Sep 29, 1969 20:03:32.8	2 SM	9
Kaminuma, 1966	Table 3b	Mar 09, 1957 14:22:27 Mar 01, 1964 08:18:56.4 Nov 11, 1964 13:17:37.5 Nov 11, 1964 19:06:57.1 Dec 17, 1964 05:18:34.0 Mar 03, 1965 19:29:16.1 Mar 05, 1965 13:42:44.1	2 SM	7

TABLE 1 (CONTINUED)

REFERENCE	SOURCE OF INFORMATION	EVENTS STUDIED	MEASUREMENT METHOD	NUMBER OF PATHS
Knopoff et al., 1966	Figures A1 thru A16	Oct 16, 1960 19:55:42.2 Oct 27, 1960 05:25:03.6 Oct 28, 1960 04:18:41.9 Oct 28, 1960 13:18:14.3 Oct 29, 1960 13:26:10.0 Nov 06, 1960 04:38:16.7 Jan 19, 1961 17:22:16.9 Mar 07, 1961 06:43:10.6 Mar 09, 1961 03:59:08.7 Mar 28, 1961 21:01:56.2 Apr 04, 1961 09:46:36.6 Apr 06, 1961 01:33:46.9 May 06, 1961 16:04:33.1 May 07, 1961 15:40:52.5 May 14, 1961 15:08:04.2 May 14, 1961 15:38:07.5	3 SM†	16
Knopoff et al., 1967	Figures 1 thru 6	Oct 29, 1960 13:26:10.0 Jun 11, 1961 05:10:26.3 Aug 30, 1961 03:35:02.7 Nov 29, 1962 19:06:37.6 Feb 22, 1963 07:10:28.0 Mar 08, 1963 02:44:31.5	3 SM†	8
Knopoff et al., 1970	Figure 2	Feb 22, 1965 20:46:36.0 Feb 22, 1965 21:22:34.3 Apr 11, 1965 04:59:39.3	1 SM	5
Knopoff and Schlue, 1972	Figure 3	Nov 12, 1965 Mar 07, 1966 Apr 20, 1966	2 SM	1
Knopoff and Vane, 1978	Table 2	Aug 07, 1972 09:24:15 Sep 09, 1972 02:44:03	2 SM	3
Kuo et al., 1962	Figures 10 thru 23, and 26	Jan 15, 1958 19:14:29 Feb 22, 1958 10:50:23. Mar 20, 1958 01:38:04 Apr 12, 1958 11:46:58 Sep 04, 1958 21:51:08 May 24, 1959 19:17:40 Oct 27, 1959 06:52:50 Dec 27, 1959 15:52:55 Feb 08, 1960 12:45:34 Mar 22, 1960 02:31:17 Mar 23, 1960 00:23:22 Apr 15, 1960 03:25:36 Jun 20, 1960 02:01:08 Aug 09, 1960 07:39:22.6 Oct 07, 1960 15:18:30.8 Nov 09, 1960 10:43:43.1	1 SM 2 SM	14 2
Landisman et al., 1969	Figure 13	Apr 29, 1963 21:44:17.2 Jun 24, 1963 04:26:37.9 Apr 04, 1964 04:54:01.7	2 SM	3
Leeds, 1975	Table II	Mar 29, 1965 10:47:37.6 Jul 29, 1965 08:29:21.2 Oct 01, 1965 08:52:04.4 Nov 12, 1965 17:52:27.6 Feb 10, 1966 14:21:11.1 Jul 04, 1966 18:33:37.1	1 SM	7
Levshin et al., 1966	Table 2	'Kamchatka and Kuril Islands shocks'	2 SM	1
Liao, 1981	Tables 15 and 23	Sep 19, 1967 10:56:08.8 Sep 25, 1968 10:38:38	1 SM 2 SM	4 1
Lyon-Caen, 1980	Figures 6 thru 15	May 06, 1976 20:00:12.5 Sep 15, 1976 03:15:18.7 Sep 15, 1976 09:21:18.6	1 SM	25
Mitchel, 1977	Figure 10	information not available	2 SM	2
Mitrovas, 1977	Tables 2A and 2B	Jan 02, 1974 10:42:29.9 May 09, 1974 23:23:25.2 Oct 23, 1974 06:14:54.8 Nov 09, 1974 12:59:49.8 to be continued	2 SM	14

(TO BE CONTINUED)

TABLE 1 (CONTINUED)

REFERENCE	SOURCE OF INFORMATION	EVENTS STUDIED	MEASUREMENT METHOD	NUMBER OF PATHS
Mitrovas, 1977 (continued)		continued Jan 19, 1975 08:00:24.3 Feb 07, 1975 04:51:44.0 Mar 13, 1975 15:26:42.5 Mar 27, 1975 05:15:06.2 May 10, 1975 14:27:40.5 Jun 16, 1975 22:35:23.2 Jul 10, 1975 18:29:16.0 Oct 28, 1975 06:54:22.4		
Moazami-Goudarzi, 1974	Table 4	9 earthquakes (origin time information not available)	2 SM	1
Mueller and Sprecher, 1978	Figure 2	Jul 03, 1973 16:59:35.1	2 SM	1
Noponen, 1966	Figure 5	Feb 23, 1964 22:41:06.3 Apr 11, 1964 16:00:42.8 Apr 29, 1964 04:21:06.7 Apr 29, 1964 17:00:02.9 Apr 05, 1965 03:12:54.2	2 SM	2
Okal and Talandier, 1980	Tables 3 and 4	Dec 29, 1975 03:39:43.0 Jul 27, 1976 19:42:54.6 Jul 28, 1976 10:45:35.2 Mar 19, 1977 23:00:58.3 Jul 29, 1977 11:15:45.3 Nov 23, 1977 09:26:24.7 Feb 22, 1978 06:07:37.0 Jun 12, 1978 08:14:26.4 Nov 29, 1978 19:52:47.6 Feb 16, 1979 10:08:54.4	2 SM	4
Panza and Calcagnile, 1974	Figure 2	Feb 10, 1971 05:18:07.0	1 SM	1
Panza et al., 1978	Figure 3a	Dec 17, 1971 19:06:07.1 Oct 06, 1973 15:07:37.3	2 SM	1
Papazachos, 1964	Figures 2, 3,4,6,7,8, 9,11,12	Nov 14, 1961 04:42:26.5 Dec 03, 1961 01:00:35.2 Jan 08, 1962 01:00:24.2 Jan 30, 1962 08:34:26.8 Feb 10, 1962 19:31:56.2 Mar 05, 1962 01:50:50.6 Mar 11, 1962 02:26:05.7 Mar 12, 1962 11:40:12.8 Mar 27, 1962 21:19:29.4 Apr 04, 1962 14:02:32.2 Apr 20, 1962 05:47:55.3 May 19, 1962 14:58:13.3 May 20, 1962 15:01:20.7 Jul 24, 1962 21:08:22.6 Jul 25, 1962 04:37:50.7 Jul 30, 1962 20:18:49.3 Sep 16, 1962 03:05:33.0 Sep 18, 1962 00:29:05.2 Feb 22, 1963 21:14:06.1 Feb 24, 1963 13:34:15.7 Nov 19, 1964 09:46:17.7	1 SM	31
Papazachos, 1969	Figures 1 thru 5	Jan 11, 1963 12:12:16 Mar 07, 1963 12:16:28 May 19, 1963 01:03:04 May 23, 1963 07:43:58 May 30, 1963 06:56:09 Jul 14, 1963 05:41:44 Dec 16, 1963 01:51:31 Jan 15, 1964 21:36:05 Jan 27, 1964 01:12:24 Mar 19, 1964 09:42:35 Mar 26, 1964 13:29:56 Aug 20, 1964 03:56:29 Dec 03, 1964 03:50:01 Mar 01, 1965 21:32:12	2 SM	5
Patton, 1973	Tables III thru VII	Oct 18, 1964 09:06:26.0 Dec 03, 1964 03:50:01.2 Sep 12, 1965 22:02:34.3 Dec 19, 1965 22:06:32.7 Feb 17, 1966 11:48:00.8 Apr 06, 1966 02:59:01.7	1 SM	19

(TO BE CONTINUED)

TABLE 1 (CONTINUED)

REFERENCE	SOURCE OF INFORMATION	EVENTS STUDIED	MEASUREMENT METHOD	NUMBER OF PATHS
Patton, 1978	Figures C1 thru C8	May 11, 1967 14:50:57 Aug 28, 1969 03:58:36.7 Sep 14, 1969 16:15:25.6 Jul 24, 1971 11:43:39.3 Oct 28, 1971 13:30:56.4 Nov 12, 1972 17:56:52.9 Aug 11, 1974 20:05:30.9 Aug 11, 1974 21:21:37.1 Aug 27, 1974 12:56:01.0	1 SM	44
Payo, 1969	Figures 1, 4a, and 4b	Jun 03, 1962 15:02:26.4 Jul 16, 1962 04:49:21.5 Aug 21, 1962 18:09:06 Aug 21, 1962 18:19:33.3 Aug 25, 1962 19:58:47.9 Aug 26, 1962 16:30:47 Sep 12, 1962 20:57:00.4 Mar 24, 1963 02:07:12.8 Apr 30, 1963 18:43:14 Jun 20, 1963 19:47:41.3 Jun 26, 1963 10:27:03.1 Jul 16, 1963 18:27:18.4 Jul 15, 1968 02:01:03	1 SM 2 SM	9 6
Payo, 1970	Figures 4a 4b, and 4c	Jun 07, 1963 19:30:35.6 Jul 04, 1963 22:56:15.7 Sep 07, 1964 11:27:16.0 Apr 08, 1966 05:52:40.0 Aug 12, 1966 15:36:17.0 Sep 01, 1966 01:38:29.9 Sep 01, 1966 21:27:39.0	3 SM†	7
Payo and Ruiz de la Parte, 1974	Figures 1 and 2	events with epicenter in Alboran Sea Algeria Atlantic Ocean Morocco	2 SM	4
Proskuryakova et al., 1970	Figures 6, 7, and 8	Jun 27, 1966 10:59 Jun 28, 1966 04:26 Aug 01, 1966 21:03 Aug 07, 1966 17:36 Aug 16, 1966 19:45 Aug 18, 1966 10:33 Sep 01, 1966 11:29 Sep 15, 1966 11:51	2 SM	3
Pujol, 1982	Figures 9a thru 9e	Apr 16, 1965 23:22:19	1 SM	12
Romanowicz, 1981	Figure 16	Jul 14, 1973 13:39:29.4 Sep 08, 1973 07:25:41 May 05, 1975 05:18:46.3	1 SM	32
Romanowicz, 1982b	Table 3 Figures 10 and 17	Jun 24, 1972 15:29:22.3 Jul 14, 1973 13:39:29.4 Aug 11, 1973 07:15:38.2 Sep 08, 1973 07:25:41 Dec 28, 1974 12:11:46.6 Apr 28, 1975 11:06:43.7 Jun 04, 1975 02:24:32.9 Agu 21, 1976 21:49:52	1 SM from one event to another	9 7
Savarensky et al., 1969	Figures 3, 5, and 6	Nov 05, 1952 00:20:02 Nov 05, 1952 19:08:26 Nov 07, 1952 14:08:35 Nov 13, 1952 07:58:47 Apr 14, 1957 19:17:57 Aug 18, 1959 06:37:18 Aug 18, 1959 15:26:10 Sep 08, 1961 11:26:33 May 11, 1962 14:11:54 May 19, 1962 14:58:13 Mar 28, 1963 00:15:50 Aug 03, 1963 10:21:37 Oct 15, 1963 09:59:26 Feb 12, 1964 20:31:53 Feb 14, 1964 16:29:45	2 SM	3
Shudofsky, 1984	Table (Appendix II)	May 07, 1964 05:45:31.9 Mar 20, 1966 01:42:51.8 Mar 20, 1966 02:39:41.0 Mar 20, 1966 03:22:43.6 to be continued	1 SM	64

(TO BE CONTINUED)

TABLE 1 (CONTINUED)

REFERENCE	SOURCE OF INFORMATION	EVENTS STUDIED	MEASUREMENT METHOD	NUMBER OF PATHS
Shudofsky, 1984 (continued)		continued Mar 20, 1966 08:55:34 Mar 21, 1966 01:30:38.0 Mar 21, 1966 09:23:49.9 May 06, 1966 02:36:53.8 May 17, 1966 07:03:29.7 Oct 05, 1966 08:34:40.1 Oct 14, 1967 23:29:31.6 May 15, 1968 07:51:16.5 Dec 02, 1968 02:33:42.4 Sep 29, 1969 20:03:32.1 Apr 14, 1970 19:08:21.8 Nov 13, 1971 15:47:44 Feb 13, 1972 10:02:42.4 Dec 18, 1972 01:18:53.4 Apr 25, 1974 00:03:47 Feb 15, 1975 06:16:25.7 Mar 26, 1975 03:40:48.4 Apr 04, 1975 17:41:16.1 Jul 01, 1976 11:24:04.7 Sep 19, 1976 14:59:43.4 Jul 06, 1977 08:48:37.4 Jul 08, 1977 06:23:03.1 Dec 15, 1977 23:20:49		
Soriau-Thevenard, 1976	Figure 2a	Sep 16, 1973 21:26:53.5 Nov 24, 1973 15:22:09.8 Jun 12, 1974 17:55:08.7 Jul 13, 1974 15:57:25.2 Apr 16, 1975 01:27:18.7	2 SM	5
Soriau, 1979	Figures 7 thru 11	Feb 09, 1971 14:00:41.6 Mar 13, 1971 23:51:35.5 Dec 05, 1971 05:50:05.8 Jan 22, 1972 13:08:49.4 Apr 03, 1972 18:52:59.8 Apr 03, 1972 20:36:20.0 Jul 05, 1972 10:16:38.4 Sep 16, 1972 09:14:32.9 Oct 20, 1972 08:17:49.2 Nov 13, 1972 04:43:47.6 Jan 01, 1973 11:42:36.1 Jun 07, 1973 18:34:43.0 Jun 17, 1973 20:37:52.0 Jul 22, 1973 02:36:52.0 Sep 15, 1973 01:45:57.7 Sep 16, 1973 21:26:53.5 Nov 04, 1973 15:52:11.7 Nov 08, 1973 08:59:12.9 Jan 25, 1976 12:23:55.5 Mar 04, 1976 02:50:00.5 Aug 23, 1976 03:30:07.6 Sep 22, 1976 00:16:08.2 Feb 19, 1977 22:34:04.1 Apr 20, 1977 23:42:50.5 Jun 28, 1977 16:18:15.2 Jun 28, 1977 19:35:01.9 Jul 29, 1977 11:15:45.0	2 SM	27
Soriau and Vadell, 1980	Figures 2 thru 5	Oct 05, 1977 05:34:46.8 Dec 28, 1977 02:45:36.7 Apr 15, 1978 23:33:47.2 May 23, 1978 23:34:11.4 Nov 05, 1978 22:02:08.3 Feb 20, 1979 06:32:38.0 May 21, 1979 22:22:24.0 Jun 10, 1979 06:49:57.0 Aug 25, 1979 08:44:05.6	2 SM	8
Stuart, 1978	Figure 1	Aug 19, 1971 08:28:53.1 Oct 30, 1971 20:48:48.0 Sep 16, 1972 03:53:26.5 Sep 19, 1972 01:36:52.4 Sep 22, 1972 19:57:27.4 Sep 23, 1972 02:14:26.8 Nov 14, 1972 04:31:42.8 Nov 21, 1972 10:06:29.6 Dec 09, 1972 06:44:40.4 Dec 27, 1972 22:59:29.7 Dec 28, 1972 14:36:07.3 Mar 18, 1973 11:06:14.7 Apr 07, 1973 03:00:58.8 Sep 27, 1973 12:29:04.3 Nov 04, 1973 15:52:11.7	2 SM	15
Suarez, 1982	Table (Appendix 2)	Jul 24, 1969 02:59:20.9 Oct 01, 1969 05:05:50.0 May 15, 1976 21:55:55.0	1 SM	46

(TO BE CONTINUED)

TABLE 1 (CONTINUED)

REFERENCE	SOURCE OF INFORMATION	EVENTS STUDIED	MEASUREMENT METHOD	NUMBER OF PATHS
Thomas, 1969	Tables 6 thru 14	Dec 25, 1962 12:09:45.6 Dec 29, 1962 10:41:04.1 Mar 28, 1963 11:12:31.3 Mar 28, 1963 23:29:14.6 Mar 31, 1963 19:22:53.3 Apr 02, 1963 04:43:30.9 May 13, 1963 22:48:10.3 May 18, 1963 12:20:31.9 Jun 02, 1963 10:00:00.1 Jun 05, 1963 22:54:28.7 Jun 15, 1963 15:30:37.7 Jun 24, 1963 16:17:15.4 Jul 14, 1963 00:02:22.8 Jul 14, 1963 14:28:22.1 Aug 13, 1963 21:52:37.4 Aug 14, 1963 02:46:44.1 Sep 14, 1963 03:52:16.9 Sep 24, 1963 16:30:16.0 Oct 02, 1963 03:31:27.0 Oct 04, 1963 02:47:32.1 Oct 26, 1963 22:41:29.8 Oct 27, 1963 10:38:49.0 Oct 27, 1963 18:24:42.9 Oct 31, 1963 03:17:42.0 Nov 18, 1963 21:11:10.2 Nov 20, 1963 11:59:58.5 Jul 25, 1964 21:29:33.2 Aug 20, 1964 12:48:47.7 Oct 11, 1964 11:10:33.6 Oct 12, 1964 15:42:54.7 Oct 17, 1964 01:38:36.0 Nov 19, 1964 15:45:31.2 Dec 30, 1964 13:19:47.4 Mar 16, 1965 16:46:15.5 Mar 29, 1965 10:47:37.6	2 SM	39
Thomson and Evison, 1962	Figure 11	Aug 18, 1959 06:37:13	2 SM	1
Tubman, 1980	Figures 5 and 10	Mar 13, 1967 19:22:19.5 Mar 16, 1967 03:11:59.3 Mar 29, 1970 03:48:47.3 Jul 29, 1970 05:50:56.4	2 SM 1 SM	4 2
Weidner, 1972	Figures 2.31, 3.9 thru 3.18	May 17, 1964 19:26:16.4 Jun 02, 1965 23:40:22.5 Nov 16, 1965 15:24:40.8 May 01, 1967 07:09:03.0 Jun 19, 1970 14:25:18.4	2 SM 1 SM	2 72

The multiple-station method and the determination of phase velocity of Rayleigh waves in Japan

The method we discuss here was first used by Aki (1961), to determine the distribution of phase velocity of Rayleigh waves in Japan. He divided the region studied into seven sub-regions, each containing a group of stations, and corresponding to different geological settings. One station in each region was selected as a reference and the least squares method was applied to determine the phase velocity c_i, the direction of propagation of the wave front θ_i, and the arrival time t_i at the reference station for the i-th peak, using the equation:

$$t_{ji} = \frac{\cos \theta_i}{c_i} \Delta\theta_j + \frac{\sin \theta_i}{c_i} \Delta\varphi_j + t_i \qquad (3)$$

where t_{ji} is the observed arrival time of the i-th peak at the j-th station, θ_i is the azimuth of propagation direction of the i-th peak (measured from the north), c_i is the phase velocity for the observed peak, and $\Delta\theta_j = \theta_j - \theta_o$, $\Delta\varphi_j = \varphi_j - \varphi_o$ (θ_j, φ_j and θ_o, φ_o are respectively the latitude and longitude of the j-th station and of the reference point at each region all measured in km).

Further developments on the phase velocity distribution in Japan using this method were made by Kaminuma & Aki (1963), Kaminuma (1964) and Kaminuma (1966a, b, c,). Other phase velocity measurements using multiple-station array data were done in Italy (Calcagnile et al., 1979 and Calcagnile & Panza, 1979).

The two-station method

The first measurements of Rayleigh waves phase velocity using the two-station method were performed by Brune & Dorman (1963) for paths within the Canadian Shield. They studied waves generated by earthquakes that were selected so that the great circle path going through each station pair would pass as close to the epicenter as possible.

The routine followed to determine the phase velocity curve for each path begins with the identification of several phases from records of both stations for each event considered. These phase were plotted in a diagram relating phase number and arrival time at the station. The period of each phase can then be determined using this peak and through method. If we consider the arrival time of a given peak and trough with period T at each station, t_1 and t_2, we can calculate c(T) the phase velocity for the Rayleigh wave with period T from the relation:

$$c(T) = \frac{\Delta}{\Delta_t - (T/2\pi)\,[\Delta\varphi(T) + 2\pi\, N(T)]} \qquad (4)$$

where $\Delta t = t_2 - t_1$ if the wave propagates from station 1 to station 2 (Fig. 2); Δ is the distance between these two stations, $\Delta\varphi(T) = \varphi_2(T) - \varphi_1(T)$ (the difference in the observed phase advances $\varphi_1(T)$ and $\varphi_2(T)$ between the two stations), and N(T) is an unknown integer which must be correctly determined. It is usually determined by calculating c(T) for several trial values of N(T) at long periods, and comparing the results with previously measured or calculated values for realistic models. N(T) are then determined from the continuity of phase as a function of T.

It is generally difficult to find an event whose epicenter will be on the great circle path connecting the two stations. We, then, choose events that will be

as close as possible to such an alignement. Brune & Dorman (1963) compare the intersect angle between the great circle direction of the epicenter to the first station, with the great circle path connecting the two stations (angle θ in Fig. 2). The practice of measuring the intersect angle became a routine by other authors that applied the method. Most reports of two-station measurements made to date include information on the limit chosen for the intersect angle. Rosa (1986) suggests that this information may be useful to judge the accuracy of each measurements, and to study lateral heterogeneity effects in the areas covered by the paths. Most studies considered by Rosa (1986) show values for $\theta \leq 10^{o}$.

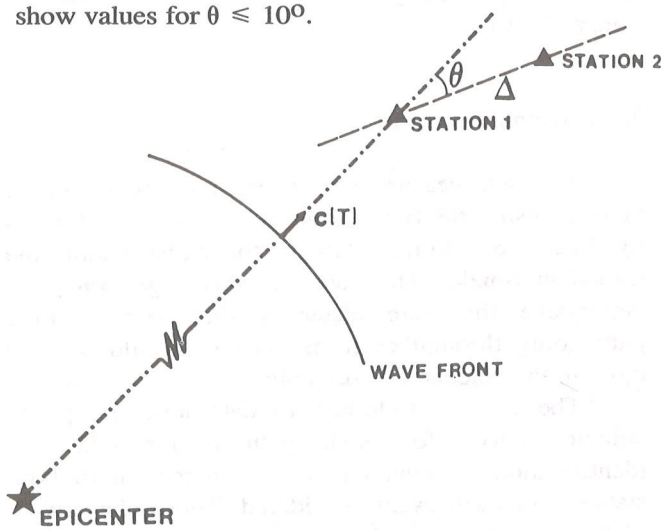

Figure 2. A station pair with spacing Δ is used to measure the phase velocity c(T) for the path between the two stations.

Figura 2. Neste caso, um par de estações, com uma distância Δ entre elas, é usado para medir a velocidade de fase c(T) entre as duas estações.

The one-station method

Brune et al. (1960) introduced the one-station method for measurement of Rayleigh wave phase velocity. In contrast with the other phase velocity measurement methods we reviewed so far, this requires the knowledge of the initial phase of the waves at the source, in order to separate the source and path effects, which was done in the other methods by using one or more additional stations assumed to share the common source effect.

The phase response curve for seismographs computed by Hagiwara (1958) was not correctly used by Brune et al. (1960), and an error of π was identified and corrected in a later paper by Brune (1962).

The correct formula for the phase velocity c(T) of Rayleigh waves with period T measured using the one-station method is given by the following equation,

$$c(T) = \frac{\Delta}{t + (T/2\pi)\,[\phi^{s}(T) - \phi^{o}(T) + \pi/4 + 2\pi\, N(T)]} \qquad (5)$$

where Δ is the epicentral distance of the observing station (Fig. 3), t is the travel time of the Rayleigh wave package arriving at the station, $\phi^{o}(T)$ is the observed phase advance corrected for the instrument response, $\phi^{s}(T)$ is the source phase advance (dependent on the focal mechanism, depth of the event and the crustal structure), and N(T) is the integer used in the unwrapping of the observed phase. This latter variable is determined using the *a priori* knowledge of 'reasonable' phase velocity values at the longest of the period range with significant signal power.

The π/4 factor corresponds to the phase shift due to the dispersion, which should be eliminated if the Fourier method is used instead of the peak-trough method for measuring φ.

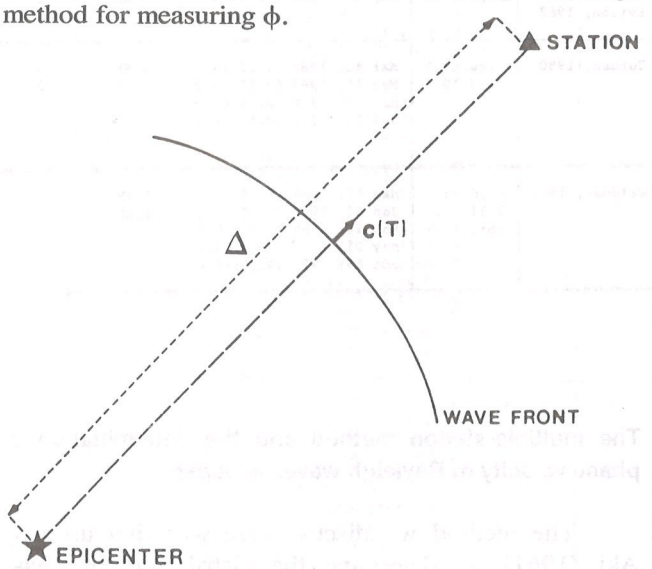

Figure 3. The one-station method gives the phase velocity for the total path between the epicenter of the event and the observing station.

Figura 3. O método de uma única estação fornece o valor de velocidade de fase para o percurso total percorrido pela onda, entre o epicentro do evento e a estação sismológica.

Weidner (1972) was the first to determine the phase velocity of Rayleigh waves, using the one-station method without assuming the focal depth and source mechanism. He used both phase and

amplitude spectra of the records for determination of the depth and focal mechanism of a pair of earthquakes sharing nearly common hypocenters but different focal mechanism. This was a major improvement over the amplitude spectra method (e.g., used by Mendiguren (1971) to study an earthquake located in the Nazca plate). In the calculations of theoretical spectra for a laterally homogeneous, vertically heterogeneous Earth model, he used the method of Saito (1967), with the oceanic model of Harkrider & Anderson (1966). The final depths and focal mechanisms determined by this method were then used to calculate the initial phase of the Rayleigh waves for use in the phase velocity determination by the one-station method.

In the phase velocity determination, Weidner (1972, 1974) used time variable filters following Landisman et al. (1969), after determination of the group velocity dispersion curves by the moving window analysis technique. Fourier analysis was used in the phase velocity calculation. This sequence of data analysis has been widely used to the present (Patton, 1978; Romanowicz, 1981, 1982a) and was also adopted (with some modifications) in the second part of our study. Weidner (1972) made an extensive error analysis for the phase velocity measurements, of which the main conclusion is that the major sources of error are the mislocation of the earthquakes and uncertainties in the origin time. According to this analysis, the error in these phase velocity measurements is about 0.02 km/sec for paths about 4000 km long, and about 0.04 km/sec for paths about 2000 km long.

Source of errors in the collected phase velocity measurements

We shall discuss now the reliability of the phase velocity measurements we have selected from the literature which are summarized in Tab. 1 and plotted in Fig. 4. Rosa (1986) reviewed the error estimates made by the authors in each reference where this information was available. These estimated were based on different assumptions regarding the major sources of error and different ways of estimation. These phase velocity measurements were made using epicentral data and origin time information of varied quality, which has improved considerably with time. Improvements on data processing techniques have also played an important role on the accuracy of phase velocity value (and also on the capability of analyzing longer periods, as was possible with the use of Fourier analysis replacing the earlier peak and trough method), together with the development of methods used to obtain the focal mechanism and depth of earthquakes

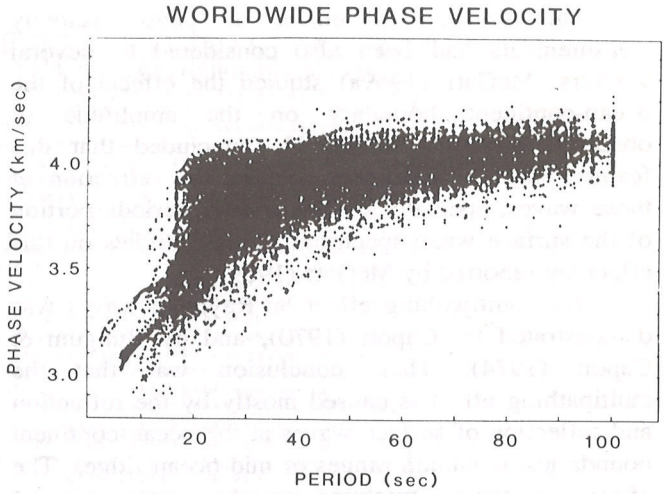

Figure 4. Plot of all the phase velocity data previously determined and included in our database.

Figura 4. Nesta ilustração, mostramos todos os valores de velocidade de fase determinados previamente por outros autores que foram incluidos em nosso banco de dados.

from body wave data. These latter developments supplied information needed to calculate the initial source phase for the application of the one-station method.

All these progresses enabled the use of the one-station method more extensively, covering large areas of the Earth. Aki & Richards (1980) pointed out that, whenever the accurate determination of the initial source phase is possible, the one-station method can provide a more accurate measurements than two and three station method. This is mainly because the effect of inhomogeneities outside the region covered by the array in the latter methods can contaminate the signal. They also discussed the advantages of the two-station method over the three-station method, because of the difference in signal coherence between the directions parallel and perpendicular to the wave front for waves propagating in a heterogeneous medium. A review of the phase velocity measurement methods and their evolution was also presented earlier by Kovach (1978).

We could then argue that our data set should be classified according to the method used for the phase velocity measurement. Unfortunately, there are complications due to the different data processing procedure, unmatched seismographic instruments, and other factors that cannot be accounted for by such a simple analysis. The errors reported by the authors we referred in this work, were evaluated using various tecniques. Rosa (1986) described these whenever the information was available.

The sources of errors in phase velocity measurements had been also considered by several workers. McGarr (1969a) studied the effects of the ocean-continent boundary on the amplitude of observed Rayleigh waves. He concluded that this feature plays a significant role on the refraction of these waves, specially on the shorter periods portion of the surface wave spectrum. Further studies on this effect are reported by McGarr (1969b).

The multipathing effect on Rayleigh waves was demonstrated by Capon (1970), and by Bungum & Capon (1974). Their conclusion was that the multipathing effect is caused mostly by the refraction and reflection of surface waves at the ocean-continent boundaries, mountain ranges or mid-ocean ridges. The effects of these structures on the phase velocity measurements of surface waves was further studied by Sobel & von Seggern (1978), who made a selection of previously measured phase velocity data from the literature (similar to the one in this work), used these data to regionalize the phase velocity values for the Earth, presenting the regionalized model in a similar fashion that we present in the next section, and performed surface wave ray tracing to study the importance of the refraction and reflection effects. They found that, for Rayleigh waves with 20 sec period, significant effects on phase velocity can be used by the refraction and/or reflection. Patton (1978) also found the focusing and multipathing of the Rayleigh waves by inhomogeneities as one of the major sources of errors in the phase velocity measurements reported in his work. He made a study of surface wave ray tracing (Patton, 1980) that showed results similar to those of the work of Sobel & von Seggern (1978). The lower boundary set by Patton (1978) who limited his study for waves with period values greater than 25 seconds is probably a good border line for such surface wave studies. He based this conclusion on the results of several numerical simultaneous he performed considering this sort of problem. Thus care should be taken when analyzing the Rayleigh wave data that might be affected by lateral heterogeneities. A careful selection of paths is the best way to avoid such complications, as emphasized by Aki et al. (1972) in their reply to the comments by McGarr (1972) on the effect of lateral heterogeneity on the Rayleigh wave spectra.

REGIONALIZATION OF THE COLLECTED DATA SET

The purpose of this part of our work is the grouping of the existing phase velocity data according to the tectonic types of their paths in order to have an initial model of global distribution of phase velocity.

The regionalization of phase velocity values for Rayleigh waves with period less than 100 sec on a global scale can have a number of applications: it can be used to detect major differences in the crustal and upper mantle structure of different areas, to obtain the focal mechanism and depth of earthquakes from the inversion of the observations of such waves generated by these events, and to calculate synthetic seismograms of surface waves. Oliver (1962), Brune (1969), Dorman (1969) and Knopoff (1972, 1983) all studied the correlation of the different regionalized phase velocity curves with the different crustal and upper mantle structure associated with several tectonic types. Sobel & von Seggern (1978) investigated the effects of lateral refraction of Rayleigh waves with 20 sec period propagating in a regionalized Earth model. The importance of regionalized phase velocity models in the study of the focal mechanism of earthquakes was demonstrated in the work of Trehu et al. (1981), who studied the focal mechanism and depth of two earthquakes located in the North Atlantic using a regionalized phase velocity model of that region. The success of the work of Trehu et al. (1981) was cited by Aki (1982), who emphasized the importance of a worldwide phase velocity model for routine determination of moment tensor and focal depth. The first attempt for calculation of synthetic seismograms of Rayleigh waves using regionalized phase velocity values was made by Aki & Nordquist (1961) who considered only the effect of dispersion. One of the latest attempts, by Yomogida (1985), includes the effect of lateral variation in phase velocity on the wave form and amplitude.

We discuss now the procedure used to regionalize the phase velocity data from the database described in the previous section and plotted in Fig. 4. We selected the period from 20 to 90 sec, with an increment of 10 sec, and the period 98 sec. The phase velocity at each of these nine period points was determined for each phase velocity dispersion curve through the interpolation of the values entered in our database. We used a cubic spline to obtain the phase velocity value c(T) at each reference period T (Hildebrand, 1974). The calculation of the spline weights suggested by Wiggins (1976) for the interpolation of points in a digitized seismogram was found appropriate in the interpolation of the phase velocity dispersion curves of our database. The interpolated data set, along with the information on the measurements, are all listed in Tab. A-1 (Appendix A).

To regionalize the interpolated phase velocity data we considered several regionalized Earth models reviewed by Soriau & Soriau (1983). They selected

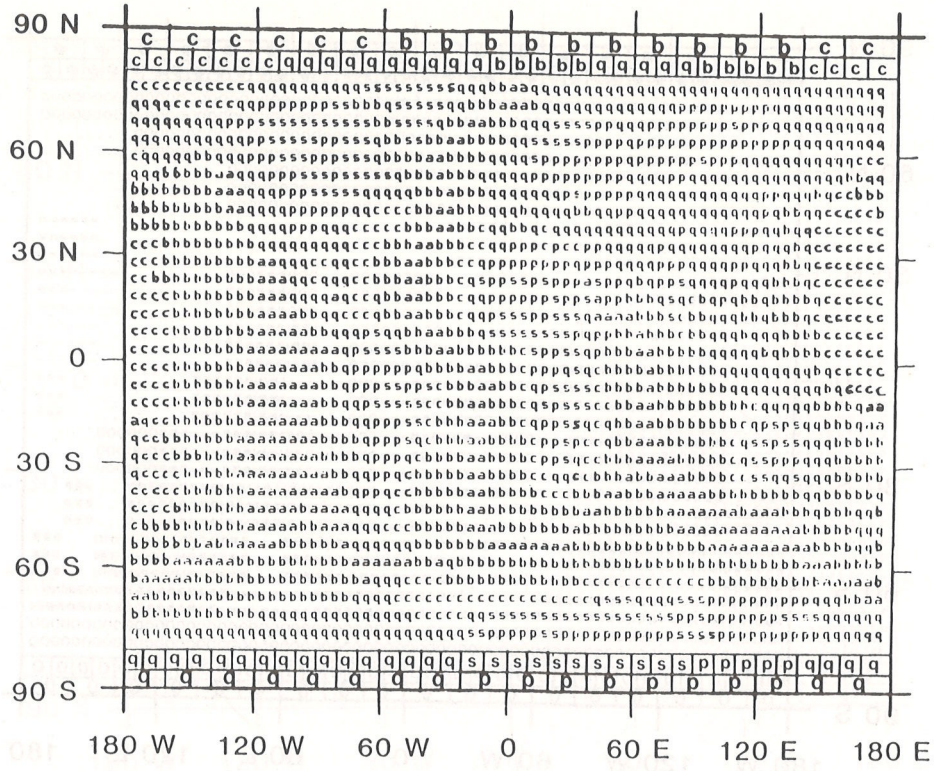

Figure 5a
Figura 5a

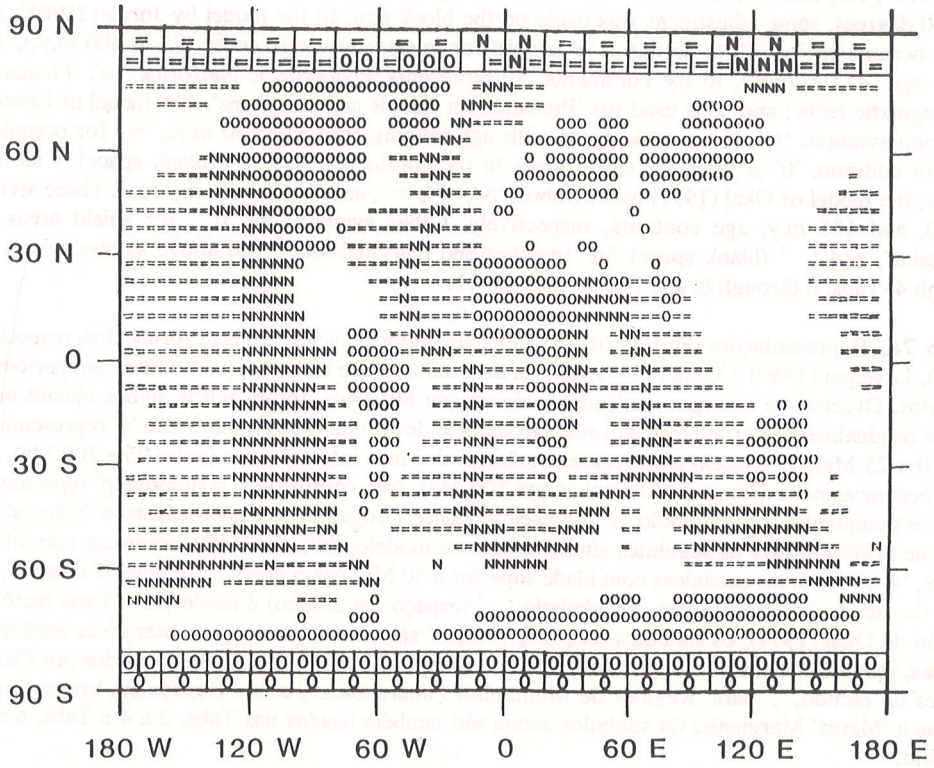

Figure 6a
Figura 6a

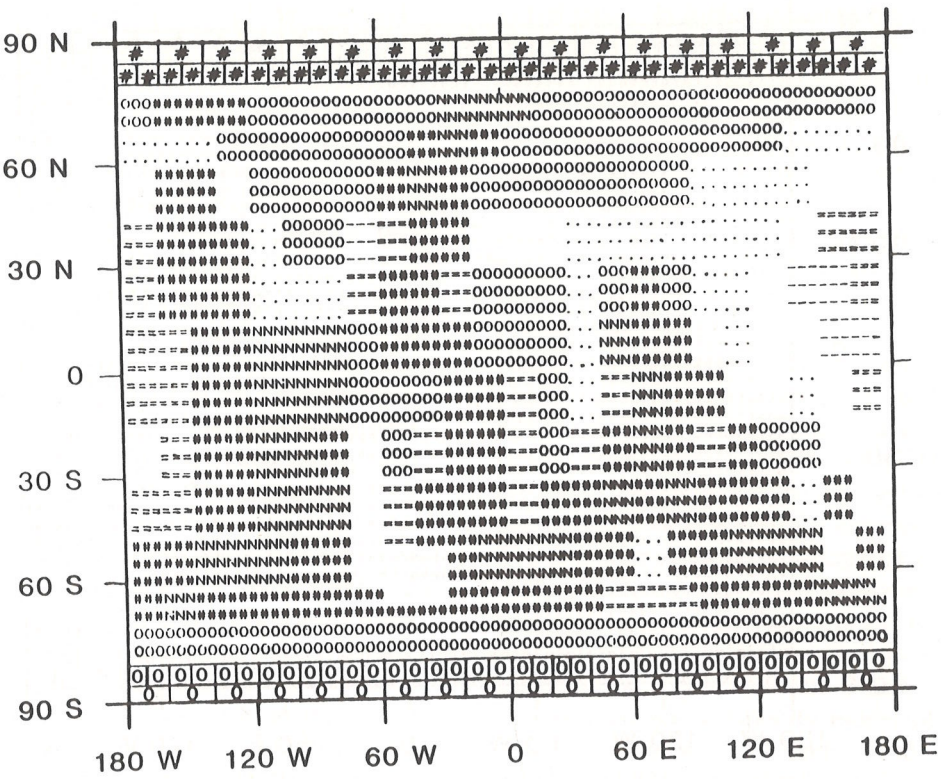

Figures 5a, 6a and 7a. Discretized representation of the regionalized Earth models of Jordan (1981), Leveque (1980), and Okal (1977) respectively, to be used for waves with period less than or equal to 50 sec. Note that, for latitudes larger than 80 degrees, some adjustment was made on the block size. In the model by Jordan (1981), symbol 'a' represents young oceanic regions (0 to 25 m.y.), 'b' is used for intermediate-age ocean (25 to 100 m.y.), 'c' corresponds to old ocean (age > 100 m.y.). In the continents, 'p' represents 'Phanerozoic platforms'; 'q', 'Phanerozoic orogenic zones and magmatic belts'; and 's' is used for 'Precambrian shields and platforms'. The model of Leveque (1980) shows the following symbols: 'N', for oceanic areas with age ranging from 0 to 30 m.y., '=' for oceanic areas older than 30 m.y.. In addition, '0' is used for shield areas in the continents, and ' ' (blank space) is used for 'tectonic areas'. Finally, the model of Okal (1977) uses symbols 'N', '#', '=', and '-' for oceanic areas. These areas are bounded by the 30, 80, and 135 m.y. age contours, respectively. Other symbols are '0' , for shield areas, '.' for 'Phanerozoic mountains', and ' ' (blank space) for 'trenches and marginal seas'. The above symbols were also used in Tabs. 2 through 4, Tabs. 6 through 8, and Figs. 9 through 11.

Figuras 5a, 6a e 7a. Representações discretas dos modelos de regionalização da Terra fornecidos, respectivamente, por Jordan (1981), Leveque (1980) e Okal (1977), que foram usados, neste trabalho, para ondas com período menor ou igual a 50 segundos. Observa-se que, para latitudes maiores que 80 graus, foram feitos alguns ajustes no tamanho dos blocos usados originalmente por aqueles autores. No modelo de Jordan (1981), o símbolo 'a' representa regiões oceânicas jovens (0 a 25 Ma), 'b' é usado para regiões oceânicas de idade intermediária (entre 25 e 100 Ma), 'c' corresponde às regiões oceânicas mais antigas (idade maior que 100 Ma). Nos continentes, o símbolo 'p' representa 'Plataformas Fanerozóicas'; enquanto que o símbolo 'q' representa 'Zonas Orogenéticas Fanerozóicas' e 'Magmatic Belts'. O modelo de Leveque (1980) mostra os seguintes símbolos em seu modelo: 'N', para áreas oceânicas com idade variando entre 0 e 30 Ma, '=', para áreas oceânicas com idade superior a 30 Ma. Além disso, o símbolo '0' é usado, em seu trabalho, para áreas de escudo nos continentes, e o símbolo ' ' (espaço em branco) é usado para 'áreas tectônicas'. Finalmente, no modelo de Okal (1977), os símbolos 'N', '#', '=' e '-' são usados para representar áreas oceânicas. Estas áreas são limitadas, respectivamente, pelos contornos de 30, 80 e 135 Ma. Outros símbolos usados por Okal (1977) são: '0', para regiões de escudo, '.' para 'Regiões de Montanhas Fanerozóicas', e ' ' (espaço em branco), que representam Trincheiras e 'Mares' Marginais. Os símbolos acima são também usados nas Tabs. 2 a 4 e Tabs. 6 a 8 e Figs. 9 a 11 deste trabalho.

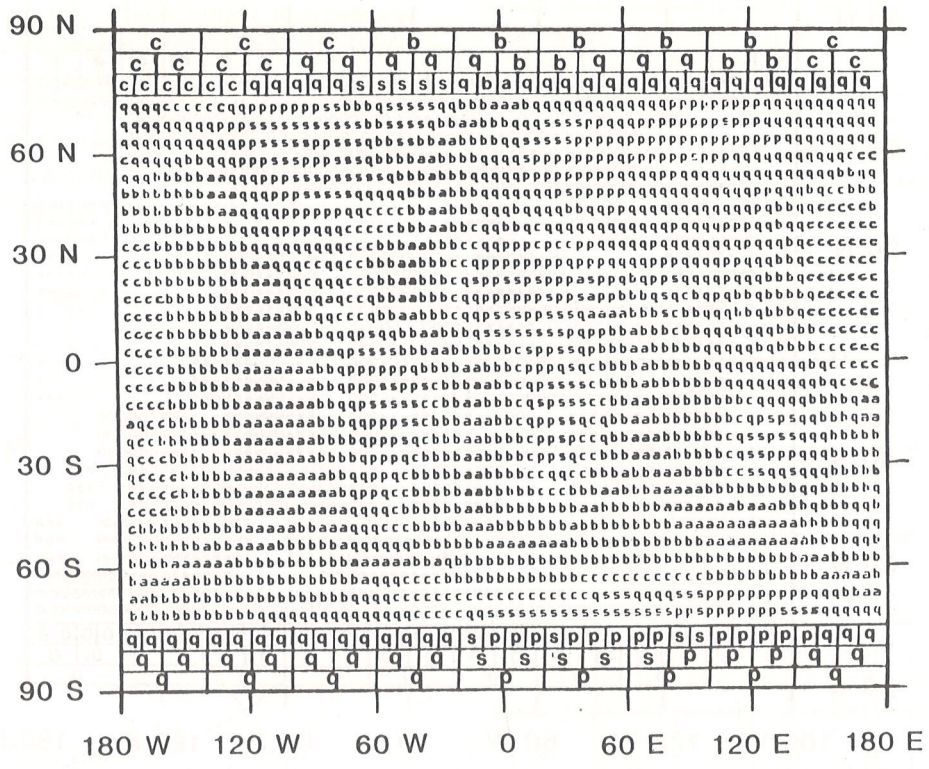

Figure 5b
Figura 5b

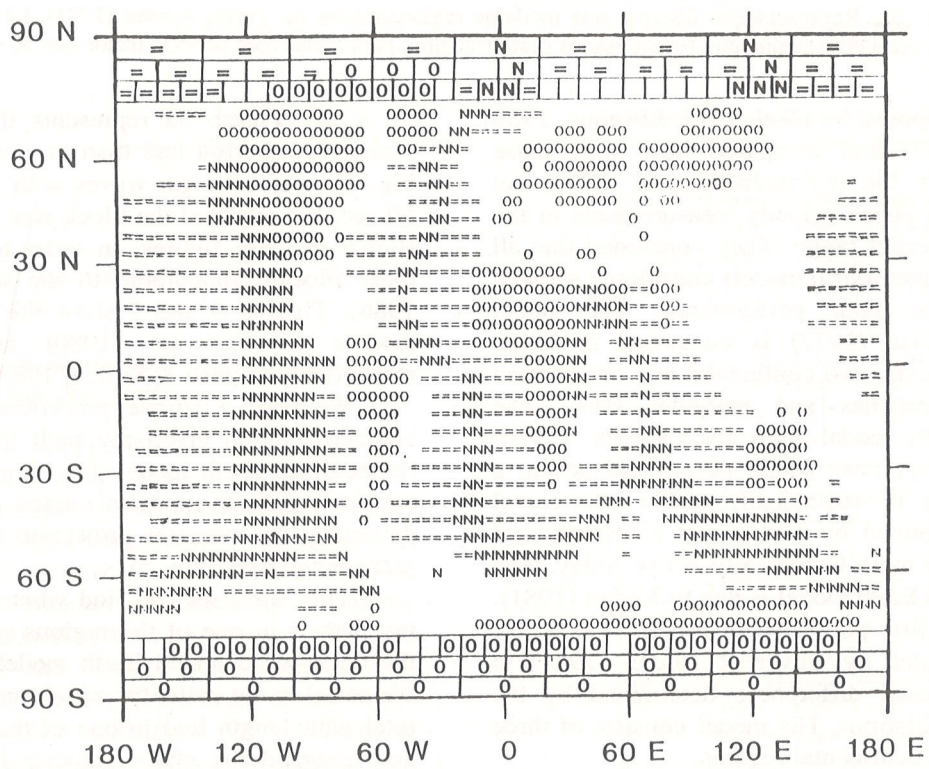

Figure 6b
Figura 6b

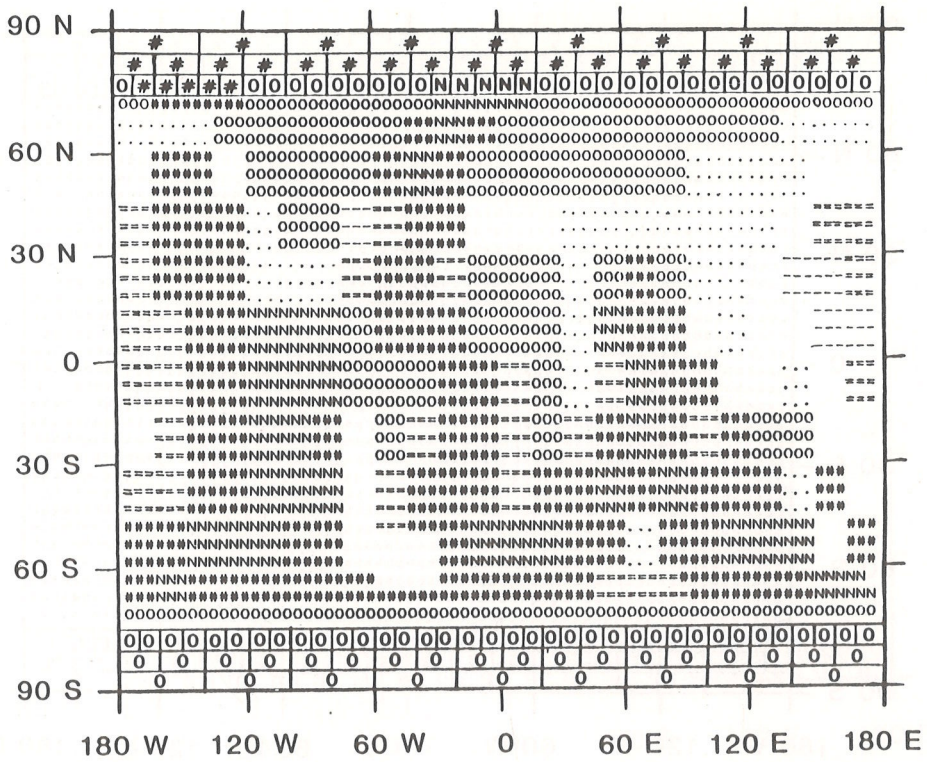

Figures 5b, 6b and 7b. Discretized representation of the regionalized Earth models of Jordan (1981), Leveque (1980), and Okal (1977) respectively, to be used for waves with period greater than 50 sec.

Figuras 5b, 6b e 7b. Representação discreta dos modelos regionalizados da Terra, Jordan (1981), Leveque (1980) e Okal (1977), respectivamente, que foram usados neste trabalho, para ondas com período maior que 50 segundos.

three models (proposed by Okal, 1977; Leveque, 1980 and Jordan, 1981) and compared how well these models behave in the regionalization of a data set composed of 296 phase velocity measurements in the 125 to 350 sec period range. They concluded that all the three regionalized Earth models considered showed approximately the same performance. The model introduced by Okal (1977) is composed of seven regions: four oceanic, two continental and one formed by areas of 'trenches and marginal seas'. The regionalized Earth model used by Leveque (1980) consists of four regions: young ocean, old ocean, a region consisting of tectonically stable continental areas, and one formed by portions of continents and oceans which are more tectonically active today. The third regionalized Earth model is due to Jordan (1981). This model was first published in Jordan (1979a, b), and was used later by Silver & Jordan (1981) to account for regional differences determined by the study of free-oscillations. His model consists of three oceanic and three continental regions.

In Fig. 5, we show the discretized version of Jordan's regionalization, using the same block size of 5^{o} x 5^{o}. Figure 5a represents the model used for waves with period less than or equal to 50 sec, while Fig. 5b was used for waves with period greater than 50 sec. We adjusted the block size at high latitudes as shown in these figures, in order to make the size of these blocks comparable to the wave lenght (Rosa, 1986). Figures 6 and 7 show the regionalized Earth models of Leveque (1980) and Okal (1977), respectively (Soriau & Soriau, 1983).

We used a simple procedure (Rosa, 1986) for characterizing a given ray path in terms of a given regionalized Earth model. For simplicity, we assumed a spherical Earth model a rotated great circle path to determine the mercator projection coordinates of each point in the path (Fig. 8).

This way, we can find what fraction of a given ray path is in one of the regions specified by each of the three regionalized Earth models described above. We selected ray paths for which more than 70% of the total path length lied in one of the specified regions, and assigned the phase velocity for the path to the region as a sample. We repeated this selection process for all periods and all ray paths for each of the three

regionalized Earth models. The resulting histogram of phase velocity for each region (shown in Rosa, 1986). Shows much narrower symmetric shape as compared to the initially skewed and broad histograms of global data. We calculated the sample mean $\bar{c}(T)$ and the square root of the sample variance $s^2(T)$ for each region, from the distribution histograms. The values of

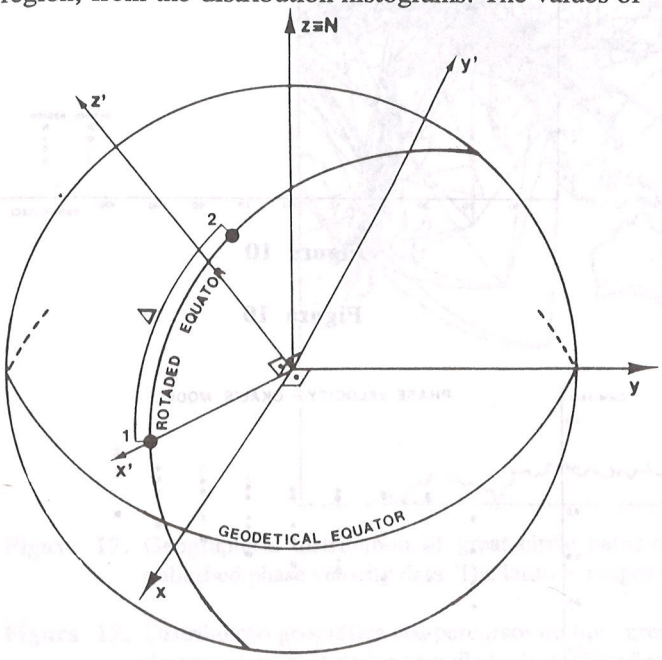

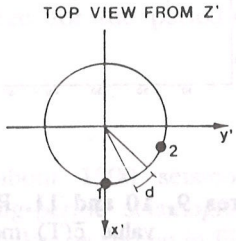

Figure 8. Coordinate systems used in tracing the great circle ray path.

Figura 8. Sistemas de coordenadas usados no traçado do percurso tipo 'great circle'.

$\bar{c}(T)$, n, and s(T) are given in Tab. 2 for the regionalized Earth model of Jordan (1981), in Tab. 3, for the model of Leveque (1980) and in Tab. 4 for the model of Okal (1977). These values were plotted in Figs. 9 through 11 for each respective model. The sample average and standard deviation for the whole data set are also included in Tab. 2.

We compared the models of Jordan (1981), Leveque (1980) and Okal (1977) in order to see which model is the most effective in performing regionalization (Rosa, 1986). This comparison was made by the use of hypothesis testing (e.g., DeGroot, 1975; Lass & Gottlieb, 1971 and Huang, 1985 for a

TABLE 2 - JORDAN'S MODEL - PHASE VELOCITY (includes also all data)

REGION / T (sec)	a	b	c	p	q	s	ALL DATA
20	3.805 38 0.053	3.882 19 0.089	3.937 23 0.045	3.580 7 0.044	3.496 103 0.141	3.631 12 0.046	3.709 426 0.199
30	3.819 41 0.044	3.959 19 0.082	4.028 37 0.037	3.828 16 0.058	3.702 197 0.173	3.876 32 0.057	3.821 736 0.155
40	3.821 40 0.040	3.965 23 0.078	4.039 46 0.033	3.968 15 0.067	3.811 190 0.143	3.996 33 0.056	3.908 786 0.122
50	3.834 39 0.042	3.960 24 0.079	4.042 45 0.034	4.034 14 0.069	3.869 177 0.105	4.033 28 0.072	3.945 745 0.101
60	3.862 36 0.027	3.975 22 0.076	4.047 45 0.035	4.068 14 0.071	3.922 155 0.090	4.064 24 0.075	3.977 676 0.088
70	3.890 34 0.028	3.994 21 0.068	4.054 45 0.039	4.102 12 0.061	3.965 132 0.080	4.097 21 0.066	4.004 633 0.079
80	3.922 31 0.028	4.015 17 0.062	4.068 45 0.042	4.119 12 0.069	4.003 114 0.067	4.121 19 0.066	4.031 581 0.073
90	3.958 31 0.027	4.044 16 0.065	4.092 43 0.045	4.146 10 0.089	4.036 84 0.057	4.146 18 † 0.069	4.058 435 0.068
98	3.985 28 0.027	4.082 12 0.066	4.120 41 0.034	4.165 9 0.103	4.076 40 0.052	4.193 5 † 0.103	4.084 261 0.064

† paths containing more than 40% of their portion inside the region were used in the indicated cases

TABLE 3 - LÉVÊQUE'S MODEL - PHASE VELOCITY

REGION / T (sec)	N	=	0	
20	3.766 54 0.136	3.933 57 0.075	3.610 61 0.117	3.495 57 0.163
30	3.800 72 0.081	4.008 78 0.065	3.846 123 0.073	3.656 149 0.169
40	3.832 70 0.073	4.020 97 0.052	3.968 126 0.084	3.778 162 0.133
50	3.859 68 0.080	4.023 95 0.051	4.007 104 0.084	3.856 163 0.091
60	3.888 62 0.083	4.030 94 0.050	4.035 89 0.087	3.910 139 0.069
70	3.918 57 0.083	4.038 93 0.051	4.062 79 0.081	3.950 119 0.054
80	3.958 52 0.081	4.058 88 0.044	4.088 67 0.073	3.988 110 0.048
90	3.969 39 0.052	4.083 81 0.043	4.122 45 0.073	4.020 72 0.046
98	3.994 33 0.036	4.111 61 0.040	4.131 24 0.086	4.062 28 0.047

TABLE 4 - OKAL'S MODEL - PHASE VELOCITY

REGION / T (sec)	N	#	=	- †	0	.	/
20	3.841 32 0.078	3.795 37 0.212	3.987 8 0.022	3.914 8 0.038	3.585 60 0.081	3.534 39 0.170	3.555 35 0.218
30	3.855 36 0.065	3.927 41 0.114	4.042 15 0.028	4.032 14 0.035	3.834 153 0.073	3.621 110 0.162	3.733 74 0.160
40	3.858 37 0.063	3.955 40 0.090	4.038 20 0.029	4.045 17 0.033	3.962 156 0.071	3.738 113 0.120	3.853 68 0.118
50	3.872 38 0.062	3.965 36 0.072	4.033 19 0.034	4.051 17 0.035	4.017 139 0.072	3.828 116 0.091	3.897 65 0.095
60	3.890 35 0.057	3.977 35 0.069	4.035 19 0.036	4.054 17 0.036	4.048 117 0.075	3.894 103 0.080	3.943 56 0.073
70	3.916 31 0.054	3.996 33 0.064	4.039 19 0.038	4.060 17 0.039	4.076 103 0.068	3.939 93 0.070	3.973 51 0.062
80	3.946 27 0.055	4.026 31 0.058	4.052 19 0.042	4.074 17 0.039	4.104 87 0.057	3.985 87 0.061	3.998 46 0.060
90	3.981 27 0.054	4.054 28 0.043	4.082 17 0.031	4.103 14 0.046	4.141 56 0.062	4.026 56 0.044	4.027 36 0.060
98	4.002 24 0.047	4.089 13 0.039	4.105 16 0.032	4.135 13 0.031	4.150 32 0.076	4.057 23 0.054	4.086 21 0.041

† paths with more than 40% of their length inside this region were used

recent geophysical application). For all three regionalization models, we tested the hypothesis that any two regions may have the same mean and variance. The results proved that the performance of all these modes is about the same. We then decided to use Jordan's (1981) model in our analysis of new phase velocity data in the second part of our study, summarized in the following section.

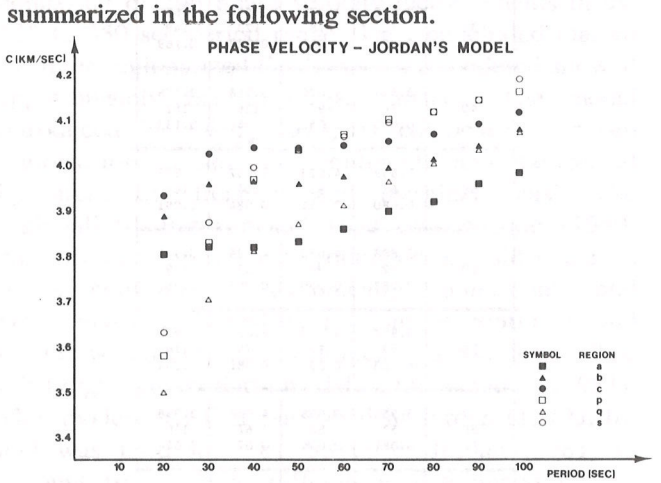

Figure 9

Figura 9

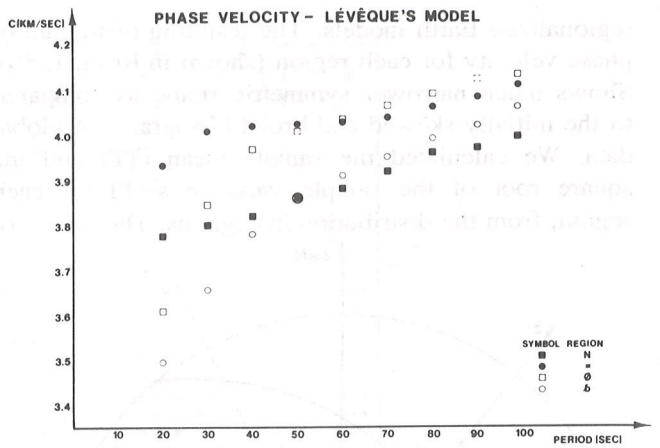

Figure 10

Figura 10

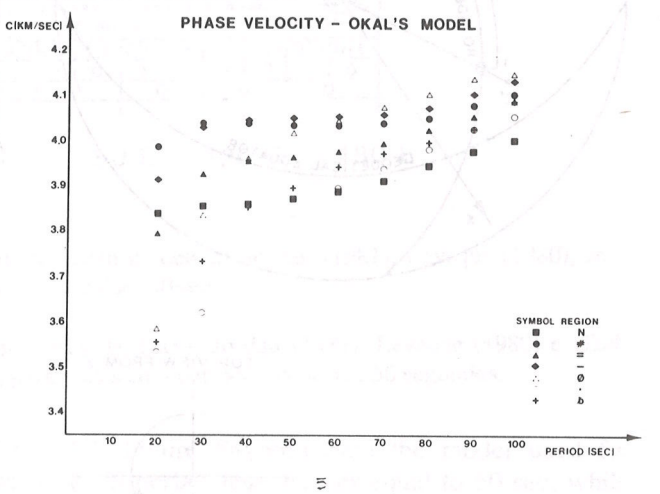

Figures 9, 10 and 11. Plot of the average phase velocity value $\bar{c}(T)$ measured for each region of the Earth models shown in Figs. 5, 6 and 7, respectively.

Figuras 9, 10 e 11. Gráfico do valor médio de velocidade de fase, $\bar{c}(T)$, medido para cada uma das regiões dos modelos regionalizados da Terra mostrados, respectivamente, nas Figs. 5, 6 e 7.

ADDITIONAL PHASE VELOCITY MEASUREMENTS

As can be seen in Fig. 12, where we show the great circle paths of the collected data for 50 seconds, the coverage of our compiled data set is far from ideal in many parts of the Earth. In order to remedy the situation, we decided to apply the one-station method to an additional set of earthquakes, for which source parameters have been determined using the body waveform data. Our work more than doubled that

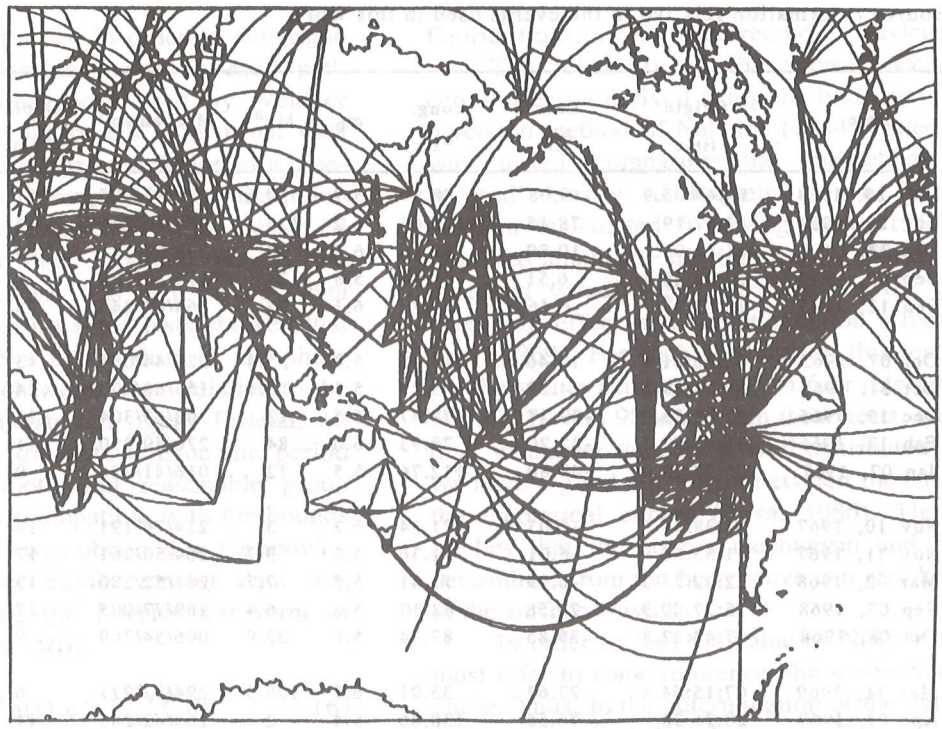

Figure 12. Geographical distribution of great circle paths corresponding to the references period 50 sec of our database of published phase velocity data. The latitude ranges from 75°N to 70°S in the map.

Figura 12. Distribuição geográfica dos percursos do tipo 'great circle', correspondentes ao período de referência de 50 segundos de nosso banco de dados compilado de publicações anteriores. A latitude varia, neste mapa, entre 75°N e 70°S.

number of paths for which the phase velocities of Rayleigh waves are measured for the period range considered.

Data processing

We used a set of about 1500 seismograms obtained by the vertical long-period seismograph of the WWSSN from 45 earthquakes as shown in Fig. 13. Their epicenter information is listed in Tab. 5. The focal mechanisms and depths of these earthquakes were obtained by a number of authors (Bergman & Solomon, 1984, 1985; Bergman et al., 1984, 1985; Bergman, 1986; Huang, 1985; Huang et al., 1986; Jemsek et al., 1986), who used a computer program developed by Nabelek (1984) for fitting the synthetic teleseismic P and SH waveform to the observed. Fortunately, the new epicenters are conveniently located so that their paths to WWSSN stations cover areas which were not covered well in earlier studies, such as the Indian Ocean, South America, South Atlantic, and western Africa regions (Fig. 12). The above authors have also chosen earthquakes with epicenters in oceanic areas, which provide records of waves that travelled a considerable part of their paths on a simple oceanic structure, which also helped to provide records of fundamental mode Rayleigh waves relatively uncontaminated by other modes.

The above set of seismograms was selected based on the overall quality of the record which was examined on a microfiche viewer. We avoided those records which showed modulated amplitude. Beating was more frequently observable for shorter period waves. The time window we selected for our study was determined from the range of arrival time corresponding to the range of group velocity curves of Oliver (1962). The end of the window was, in many cases, placed at the appearance of the beating phenomenon.

The above seismograms were then digitized, in the window set for each case, and corrected for the eventual rotation of the seismogram with relation to the coordinate system of the digitizer and to account for the helical movement of the recording drum (James & Linde, 1971).

Finally, the corrected amplitude and time pair for each digitized point, was used in the interpolation process to determine the amplitude at every second (a(t)). The interpolation method used, based on the cubic spline interpolation, was shown by Wiggins (1976) to be the most appropriate for the interpolation of digitized seismograms.

In the next step of the data processing, we have applied the moving window analysis of Landisman et

Table 5. Source information relative to the events used in this work.

Event no.	Date	Origin time	Lat. °N	Long. °E	m_b	M_o[a]	Mechanism[b]	Depth[c] (km)	Water layer[d] (km)	Ref.[e]
1	May 25, 1964	19:44:05.9	-9.08	88.89	5.7	9.6	177/87/005	17	5	iii
2	Aug 25, 1964	13:47:19	78.15	126.65	6.2	125	171/46/277	5	2	vii
3	Oct 23, 1964	01:56:05.1	19.80	-56.11	6.2	50	283/54/151	30	5	iv
4	Sep 09, 1965	10:02:25.7	6.51	-84.44	5.8	24	173/88/160	8	2	ii
5	Sep 12, 1965	22:02:37.7	-6.46	70.76	6.1	33	263/44/246	18	4	ii
6	Oct 07, 1965	03:36:01.4	12.46	114.45	5.8	5.4	220/44/085	3	4	iv
7	Oct 31, 1965	17:24:09.5	-14.22	95.27	5.3	6.1	165/68/009	24	5	iii
8	Dec 19, 1965	22:06:33.0	-32.24	78.87	5.5	13	300/68/304	11	4	i
9	Feb 17, 1966	11:47:57.3	-32.20	78.93	6.0	84	276/59/290	11	4	i
10	Jan 07, 1967	00:27:23.0	-48.80	112.76	5.5	12	016/41/236	9	2	ii
11	Nov 10, 1967	18:38:34	-6.03	71.34	5.2	3	234/76/191	18	3	ii
12	Nov 11, 1967	11:55:56	-6.01	71.36	5.3	3.7	264/50/261	17	2	ii
13	Mar 02, 1968	22:02:24.2	-6.09	71.41	5.5	7.7	284/52/280	13	1	ii
14	Sep 03, 1968	15:37:00.3	20.58	-62.30	5.6	6.4	169/77/005	27	5	iv
15	Oct 08, 1968	07:43:22.8	39.85	87.74	5.8	22.8	006/54/269	9	4	i
16	Mar 31, 1969	07:15:54.4	27.61	33.91	6.1	106.3	294/37/271	6	n.a.	v
17	Apr 07, 1969	20:26:30	76.55	130.86	5.4	2	163/42/285	11	n.a.	vii
18	Aug 08, 1969	11:08:13.2	-47.76	-15.66	5.7	15	008/67/215	7	3	ii
19	Sep 20, 1969	05:08:57.8	58.35	-32.08	5.6	15	023/42/261	2	2	vi
20	Jan 21, 1970	17:51:37.4	7.03	-104.24	6.1	140	332/41/106	6	3	ii
21	Mar 31, 1970	18:18:28.0	-3.78	69.70	5.5	8	043/83/187	13	4	ii
22	Apr 25, 1970	03:43:31	-6.29	69.84	5.1	1.6	248/85/192	11	4	ii
23	May 09, 1971	08:25:01.1	-39.78	-104.87	6.0	53	025/46/104	9	4	ii
24	May 31, 1971	03:46:50.6	72.21	1.09	5.5	6.8	051/51/284	2	3	vi
25	Jun 26, 1971	19:27:11	-5.18	96.90	5.9	54	014/67/019	29	5	iii
26	Sep 30, 1971	21:24:10.8	-0.45	-4.89	6.0	10	081/59/074	13	5	iv
27	May 02, 1972	06:56:23.2	5.22	-100.32	5.9	18	332/49/280	11	3	ii
28	May 21, 1972	06:01:54.3	-27.10	174.97	5.6	4.8	333/72/157	13	4	iv
29	Oct 20, 1972	04:33:49.9	20.60	-29.69	5.7	28	250/80/170	18	5	iv
30	Apr 26, 1973	20:26:27	20.05	-155.16	5.9	37	087/64/346	41	1	iv
31	Aug 30, 1973	19:50:03.9	7.15	84.33	5.8	3.7	290/52/118	27	4	iii
32	Jul 01, 1974	23:11:14.5	-22.57	-10.68	5.5	3.3	068/29/092	3	4	ii
33	Nov 20, 1974	13:21:41.6	-53.59	-28.26	5.8	6.6	298/87/005	5	5	iv
34	Sep 11, 1975	22:00:01.3	7.05	-104.18	6.3	11	307/44/093	5	3	ii
35	Sep 19, 1975	03:37:11	-34.74	81.88	5.9	48.5	241/63/275	18	3	i
36	Mar 29, 1976	05:39:36.3	3.96	-85.88	5.8	92	199/82/181	8	3	ii
37	Aug 30, 1976	08:37:54.4	1.03	147.56	5.8	24	334/77/173	25	5	iv
38	Nov 02, 1976	07:13:17	-29.36	77.65	5.8	76.4	230/37/282	14	4	i
39	Feb 05, 1977	03:29:19	-66.49	-82.45	6.1	40	003/43/073	14	4	iv
40	Jun 28, 1977	19:18:36	22.68	-45.11	5.9	11	001/44/255	2	4	vi
41	Aug 26, 1977	19:50:02.3	-59.54	-20.59	6.3	540	091/85/175	9	5	ii
42	Oct 17, 1977	17:26:40.4	-27.93	173.13	6.2	200	274/78/010	13	3	iv
43	Dec 13, 1977	01:14:20.5	17.33	-54.91	5.7	44	240/60/050	22	5	iv
44	Mar 24, 1978	00:42:36.7	29.68	-67.45	6.0	20	331/46/089	8	5	iv
45	Jan 28, 1979	19:45:21	11.92	-43.70	5.7	6.3	020/46/270	2	4	vi

a. Seismic moment x 10^{24} dyne.cm (units equivalent to 10^{17} N.m); b. Focal mechanism: strike, dip and slip angles (in degrees), according to the convention of Aki & Richards (1980); c. Centroid depth (km below seafloor); d. Approximate water depth at the epicentral region; e. Reference body-wave studies: i) Bergman et al. (1984, 1985; ii) Bergman & Solomon (1984); iii) Bergman & Solomon (1985); iv) Bergman (1986); v) Huang (1985); vi) Huang et al. (1986); vii) Jemsek et al. (1986).

al. (1969). This was performed in order to determine the group velocity dispersion curve of each path studied. This technique has been used by Weidner (1972), Forsyth (1973), and others. The usual data treatment procedure also included the design of a time-variable filter from these group velocity dispersion curves, to eliminate contamination of the observed spectra by waves other than Rayleigh waves. We chose, however, not to use this step in our data processing sequence, because some tests showed that it was common to have a phase shift in the phase spectra resultant from such windowing, relative to the phase spectrum of the undistorted signal. Instead, we eliminated (Rosa, 1986) the data outside the period bands for which a smooth and reasonable group velocity dispersion curve (compatible with the bounds supplied by Oliver, 1962) was obtained in the moving window analysis. Further elimination of data was necessary while checking the Fourier transform of each digitized seismogram (a(t)),

$$A_{obs}(T)\, e^{-i\varphi^o(T)} = \int_{t_1}^{t_2} a(t)\, e^{-2\pi i t/T}\, dt \qquad (6)$$

where t_1 and t_2 are the time limits of the window. We have plotted the observed amplitude $A_{obs}(T)$ and phase delay $\varphi^o(T)$ (after application of the formulas of Hagiwara, 1958, for the instrument response correction) for each path, and eliminated the period range in which phase spectra varied irregularly (Rosa, 1986). At this point, a total of 1242 seismograms remained from our original set of about 1500.

In the next step of our data analysis (Rosa, 1986), an extensive use was made of a formula for the calculation of the vertical component of the fundamental mode Rayleigh wave spectrum for a point source buried in a laterally homogeneous layered medium that had been derived by Saito (1967). This step has been used by several authors (e.g. Weidner, 1972; Forsyth, 1973; Patton, 1978, and others) in the determination of phase velocity by the one-station method, in which the source phase advance, $\varphi^s(T)$ is calculated for a given set of source parameters, and the source depth. The phase velocity c(T) for the path between a given station and the corresponding epicenter for each of those earthquakes (Tab. 5) can then be determined from the observed phase advance $\varphi^o(T)$ that has been corrected for the instrument response,

$$c(T) = \frac{\Delta}{t + (T/2\pi)\,[\varphi^s(T) - \varphi^o(T) + \pi/4 + 2\pi\, N(T)]} \qquad (7)$$

Here, t represents the starting time for calculating the Fourier transform for each record of Rayleigh waves.

The reliability of the source mechanism and centroid depth derived using the body wave modelling inversion method of Nabelek (1984) (listed in Tab. 5) was tested comparing the theoretical amplitude spectral density of Rayleigh waves in a layered medium (calculated following Saito, 1967) with the observed amplitude spectral density (Rosa, 1986). The observed values were corrected for the geometrical spreading effect and the attenuation effect following Tsai (1969). For each earthquake, this test was made for the whole azimuth range, at four reference periods: 30, 50, 70 and 98 sec. From these tests, we could see that, whenever the data is well distributed in azimuth, we have a good agreement between the calculated and the theoretical curves (Rosa, 1986). The agreement implies that the source mechanism and focal depth determined from the body wave can also be applicable to the surface waves.

In order to find the value of N(T) in eq. (7), one must refer to some reference phase velocity dispersion curve. Thus, in the determination of the value of N(T), we made use of the phase velocity estimate for the particular path calculated using the initial model derived in the previous section. We used the regionalized Earth model by Jordan (1981), with the values listed in Tab. 2 to select the value of N(T) which gives the closest predicted value of c(T). The above upwrapping procedure gave, in general, satisfactory result except for the shortest periods, and provided us with the phase velocity data for 1242 new paths in addition to the data from the first part of this work. These data are all listed, along with the corresponding group velocity values for each period, in Tab. B-1 (Appendix B) of this paper.

Error analysis

The data processing procedure used in this section are very similar to those used by Weidner (1972), Forsyth (1973), Patton (1978), Romanowicz (1981, 1982b), Suarez (1982), and Pujol (1982). The portions of the data processing in our study that differ from the earlier works are: avoiding the use of time-variable filter, and unwrapping of the observed phase spectra using an automated process based on the initial model. There may be differences in the errors in phase velocity due to differences in uncertainties in the focal mechanism and depth of each earthquake. These uncertainties depend on several factors. Different types of fault mechanism and depth can cause different sources of uncertainty. For example, it seems that the strike-slip events cause more problems with the strike uncertainty, due to the four-lobed azimuthal variation

of the radiation pattern. This causes phase changes more often than, for example, dip slip mechanism. The ideal approach would be the simultaneous inversion, in which both the phase velocity distribution and the source parameters are adjusted to improve the agreement between the observed and predicted amplitude and phase spectra. Such an approach was taken by Weidner (1972), Patton (1978) and others.

The errors in our phase velocity data are probably of the same magnitude as those in Forsyth (1973) (at most 0.06 km/sec), and better than most works we reviewed so far, but they are by no means comparable to the error level achieved by a work such as Weidner (1972), who accomplished an almost complete separation of source and propagation effects on these waves and the accuracy of phase velocity as good as $\pm$ 0.02 km/sec in the period range 20-100 sec.

Some of the event-station pairs we studied were also used by previous workers, whose work we reviewed above. We have searched our database and found that we had 14 pairs already studied by other authors. Rosa (1986) checked those data and found that despite some difference in the focal mechanism and depth used by our study and theirs, there is a good agreement between the phase velocity values in most cases (less than 0.05 km/sec).

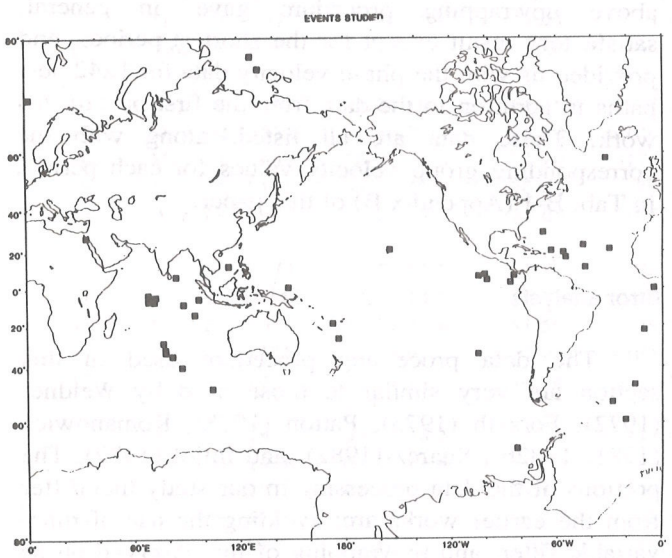

Figure 13. Geographic distribution of the earthquake studied in this work.

Figura 13. Distribuição geográfica do epicentro dos eventos estudados neste trabalho.

Regionalization of the group velocity data

In the work described above, we used the group velocity measured for each path as a guide to determine which portions of the Rayleigh wave spectrum were suitable for the phase velocity measurement. These data will be used here to determine regional variation of group velocity for the period range 20 to 100 sec, in the same fashion we analyzed the phase velocity data compiled from the literature. To achieve this objective, we grouped these data using the same three regionalized Earth models as discussed for the phase velocity case, with their discretized version shown in Figs. 5 through 7 for the models of Jordan (1981), Leveque (1980), and Okal (1977), respectively. This time, we selected ray paths for which more than 40 percent of the total path length lies in one of the specified regions, instead of the 70 percent limit used for the phase velocity estimation for each region (because, in this case, the path lenghts are much longer than in the phase velocity study).

TABLE 6

JORDAN'S MODEL - GROUP VELOCITY (includes also all data)

REGION / T (sec)	a	b	c	p	q	s	ALL DATA
20	3.646 51 0.170	3.544 183 0.187	3.487 20 0.174	3.072 10 0.162	3.169 51 0.177	3.194 11 0.101	3.440 414 0.237
30	3.787 95 0.126	3.770 427 0.145	3.735 55 0.177	3.336 41 0.178	3.457 184 0.199	3.452 19 0.092	3.647 1056 0.211
40	3.816 106 0.105	3.856 449 0.105	3.876 60 0.137	3.597 48 0.132	3.644 228 0.140	3.671 18 0.084	3.775 1163 0.143
50	3.802 104 0.083	3.868 444 0.090	3.901 60 0.113	3.729 49 0.065	3.733 234 0.107	3.819 18 0.068	3.824 1168 0.105
60	3.776 100 0.073	3.858 428 0.085	3.901 58 0.103	3.781 47 0.061	3.758 230 0.103	3.885 18 0.040	3.833 1137 0.094
70	3.748 96 0.065	3.832 375 0.081	3.871 53 0.089	3.792 44 0.062	3.763 218 0.100	3.903 18 0.034	3.822 1042 0.088
80	3.723 91 0.065	3.804 340 0.083	3.840 48 0.093	3.790 42 0.060	3.760 207 0.100	3.894 16 0.041	3.804 971 0.088
90	3.697 82 0.070	3.774 283 0.086	3.814 41 0.070	3.793 37 0.061	3.747 188 0.105	3.873 12 0.057	3.783 853 0.090
98	3.681 68 0.064	3.757 224 0.086	3.787 29 0.064	3.785 30 0.063	3.751 159 0.096	3.866 10 0.075	3.769 700 0.089

TABLE 7

LÉVÊQUE'S MODEL - GROUP VELOCITY

REGION / T (sec)	N	=	U	Y
20	3.638 74 0.183	3.513 214 0.195	3.172 52 0.144	3.305 76 0.227
30	3.763 137 0.150	3.757 483 0.157	3.427 161 0.153	3.544 253 0.212
40	3.805 150 0.116	3.861 507 0.107	3.667 184 0.110	3.695 295 0.143
50	3.801 148 0.089	3.880 501 0.089	3.786 185 0.079	3.762 303 0.103
60	3.781 146 0.082	3.874 486 0.082	3.834 182 0.076	3.781 297 0.096
70	3.756 136 0.074	3.851 439 0.075	3.855 162 0.065	3.777 276 0.088
80	3.730 127 0.072	3.827 398 0.077	3.853 154 0.062	3.769 259 0.084
90	3.703 115 0.075	3.800 338 0.078	3.840 138 0.067	3.755 233 0.085
98	3.682 97 0.073	3.780 266 0.079	3.831 115 0.073	3.751 205 0.077

TABLE 8

OKAL'S MODEL - GROUP VELOCITY

REGION / T (sec)	N	#	=	-	0	.	Y
20	3.593 57 0.204	3.514 161 0.208	3.501 32 0.158	3.540 4 0.124	3.167 68 0.164	3.233 19 0.191	3.331 14 0.225
30	3.755 95 0.124	3.739 354 0.174	3.778 58 0.147	3.789 9 0.138	3.436 213 0.166	3.483 73 0.202	3.665 45 0.165
40	3.802 100 0.088	3.843 376 0.113	3.897 60 0.099	3.884 9 0.129	3.666 244 0.120	3.617 94 0.138	3.757 55 0.107
50	3.795 101 0.072	3.866 376 0.087	3.929 53 0.067	3.913 9 0.121	3.785 250 0.080	3.691 95 0.101	3.771 57 0.103
60	3.779 100 0.064	3.862 361 0.075	3.919 50 0.066	3.947 9 0.119	3.831 246 0.076	3.709 93 0.096	3.770 55 0.100
70	3.755 94 0.060	3.837 325 0.074	3.879 40 0.060	3.900 7 0.090	3.845 228 0.072	3.712 86 0.093	3.752 47 0.095
80	3.732 88 0.057	3.812 296 0.075	3.844 33 0.075	3.875 6 0.085	3.842 220 0.070	3.705 80 0.089	3.729 45 0.090
90	3.707 75 0.059	3.783 256 0.081	3.813 26 0.073	3.862 5 0.102	3.828 198 0.073	3.692 71 0.095	3.705 40 0.093
98	3.688 60 0.052	3.764 203 0.086	3.785 20 0.076	3.810 2 0.099	3.819 162 0.071	3.699 60 0.081	3.703 32 0.089

We calculated the sample mean $\bar{u}(T)$, and the square root of the sample variance $s^2(T)$ for each region, of each region, of each regionalized model. These values, together with the number of samples assigned to each region, are shown in Tabs. 6 through 8, for the regionalized Earth models of Jordan (1981), Leveque (1980), and Okal (1977), respectively. The sample average and the standard deviation for the whole data set are also shown in Tab. 6. The sample average values of Tabs. 6 through 8 are plotted in Figs. 14 through 16, respectively.

We compared the models of Jordan (1981), Leveque (1980), and Okal (1977) in the same fashion as in the phase velocity study. This time, we found that the performance of the models of Jordan (1981), and Okal (1977), have roughly the same effectiveness, in contrast with the much better performance of the four-region model of Leveque (1980), which used a much coarser grid than the others.

CONCLUSIONS

We have gathered from the literature a large amount of phase velocity data for fundamental mode Rayleigh waves with period ranging between 20 to

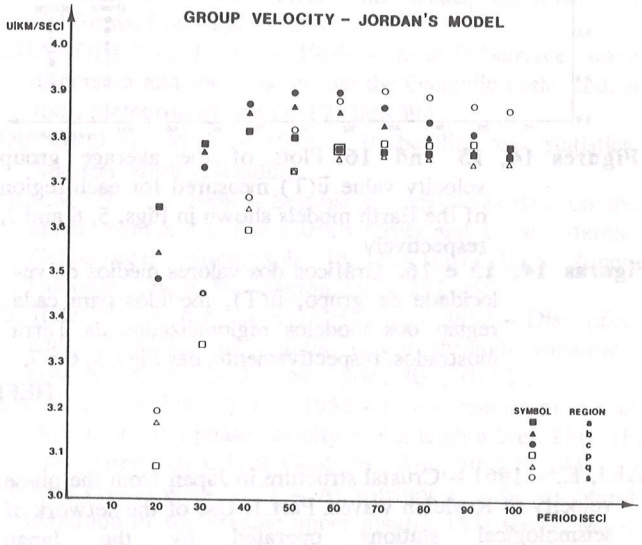

Figure 14

Figura 14

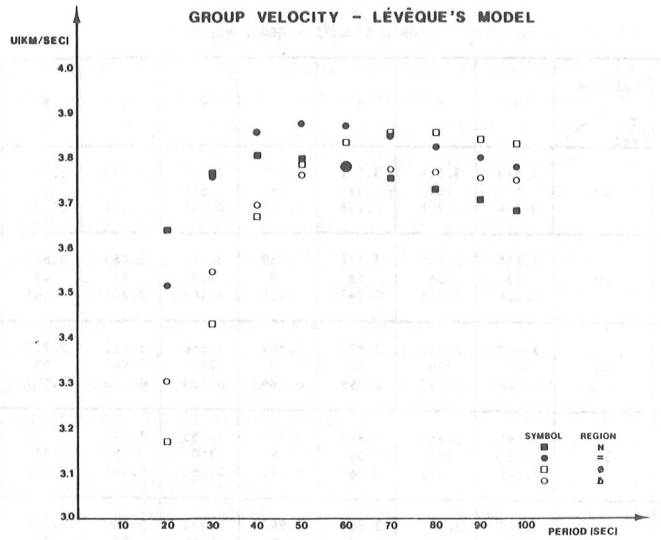

Figure 15

Figura 15

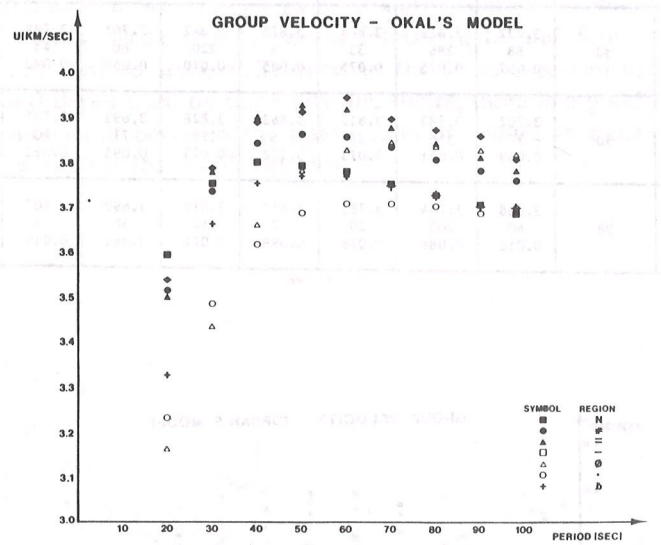

Figures 14, 15 and 16. Plots of the average group velocity value $\bar{u}(T)$ measured for each region of the Earth models shown in Figs. 5, 6 and 7, respectively.

Figuras 14, 15 e 16. Gráficos dos valores médios de velocidade de grupo, $\bar{u}(T)$, medidos para cada região dos modelos regionalizados da Terra mostrados, respectivamente, nas Figs. 5, 6 e 7.

100 sec, and organized a database of these values so that they can be effectively and routinely used for various purposes.

The collected data were used to determine the mean phase velocity for the regionalized Earth models of Jordan (1981), Leveque (1980), and Okal (1977). These values serve as an initial model used in the second part of our study, where we performed observations corresponding to Rayleigh waves generated by a set of 45 earthquakes, which had their source mechanism and focal depth determined by other authors using body-waveform data matching. The source mechanisms and focal depths agree well with the surface wave amplitude data of Rosa (1986). The newly measured phase velocities were used to increase our original database, which was more than doubled.

The three regionalized Earth models above can also be used in a variety of fields in Geophysics to study areas located anywhere on the Earth. We hope that this newly available and well-catalogued set of information will significantly increase the use of fundamental mode Rayleigh waves in the period range considered, in geophysical studies.

The group velocity database presented in this paper is also a contribution to the study of Rayleigh waves, despite the larger measurement errors than the phase velocity data.

ACKNOWLEDGEMENTS

This project was made possible at MIT by a NSF grant (EAR-8408714), and was supported at USC by DARPA contract F19628-85-K-0018 and by the Schlumberger-Doll Research Fund. J.W.C. Rosa's studies at MIT were supported by the Brazilian National Research Council (CNPq), proc. 20.1022/81, while further work done for the set up of this publication was supported by CAPES, Ministry of Education, República Federativa do Brasil.

REFERENCES

AKI, K. – 1961 – Crustal structure in Japan from the phase velocity of Rayleigh waves. Part 1: Use of the network of seismological stations operated by the Japan Meteorological Agency. Bull. Earthq. Res. Inst., **39**: 255-283.

AKI, K. – 1982 – Progress report on the determination of seismic moment tensor from long-period surface waves. Tectonophysics, **84**: 1-2.

AKI, K., MENDIGUREN, J.A. & TSAI, Y.B. – 1972 – Reply on A. McGarr's 'Comments on some papers concerning amplitudes of seismic surface waves'. J. Geophys. Res., **77**: 3827-3830.

AKI, K. & NORDQUIST, J.M. – 1961 – Automatic computation of impulse response seismograms of Rayleigh waves for mixed paths. Bull. Seismol. Soc. Am., **51**: 29-34.

AKI, K. & RICHARDS, P.G. – 1980 – Quantitative Seismology, Theory and Methods. Vols. 1 and 2, W.H. Freeman, San Francisco.

BACHE, T.C., RODI, W.L. & KARKRIDER, D.G. – 1978 – Crustal structures inferred from Rayleigh-wave signatures of NTS explosions. Bull. Seismol. Soc. Am., **68**: 1399-1413.

BALDI, P., FERRARI, G. & MANTOVANI, E. – 1979 – Evidence of rifting in the Tyrrhenian Sea observing Rayleigh wave dispersion. Bolletino di Geofisica Teorica, **21**: 94-104.

BALDI, P., GASPERINI, M. & MANTOVANI, E. – 1979 – Rayleigh wave velocities in Central Northern Italy. Annali di Geofisica, **31**: 181-196.

BERGMAN, E.A. – 1986 – Intraplate earthquakes and the state of stress in oceanic lithosphere. Tectonophysics, **132**: 1-35.

BERGMAN, E.A., NABELECK, J.L. & SOLOMON, S.C. – 1984 – An extensive region of off-ridge normal-faulting earthquakes in the southern Indian Ocean. J. Geophys. Res., **89**: 2425-2443.

BERGMAN, E.A., NABELEK, J.L. & SOLOMON, S.C. – 1985 – Correction to "An extensive region of off-ridge normal-faulting earthquakes in the southern Indian Ocean". J. Geophys. Res., **90**: 2066-2067.

BERGMAN, E.A. & SOLOMON, S.C. – 1984 – Source mechanism of earthquakes near mid-ocean ridges from body waveform inversion: implications for the early evolution of oceanic lithosphere. J. Geophys. Res., **89**: 11415-11441.

BERGMAN, E.A. & SOLOMON, S.C. – 1985 – Earthquake source mechanisms from body-waveform inversion and intraplate tectonics in the northern Indian Ocean. Phys. Earth Planet. Inter., **40**: 1-23.

BERRY, M.J. & KNOPOFF, L. – 1967 – Structure of the upper mantle under the Western Mediterranean Basin. J. Geophys. Res., **72**: 3613-3626.

BISWAS, N.N. – 1971 – The upper mantle structure of the United States from the dispersion of surface waves. PhD thesis, University of California, Los Angeles, 175 pp.

BLOCH, S. & HALES, A.L. – 1968 – New techniques for the determination of surface wave phase velocities. Bull. Seismol. Soc. Am., **58**: 1021-1034.

BOLT, B.A. & NIAZI, M. – 1964 – Dispersion of Rayleigh waves across Australia. Geophys. J.R. astr. Soc., **9**: 21-35.

BROOKS, J.A. – 1969 – Rayleigh waves in southern New Guinea II-A shear velocity profile. Bull. Seismol. Soc. Am., **59**: 2017-2038.

BRUNE, J.N. – 1962 – Correction of initial phase measurements for the southeast Alaska earthquake of July 10, 1958, and for certain nuclear explosions. J. Geophys. Res., **67**: 3643-3644.

BRUNE, J.N. – 1969 – Surface waves and crustal structure. In: The Earth's Crust and Upper Mantle. Geophysical Monograph 13, P. Hart (ed.), Amer. Geophys. Union, Washington, D.C., 230-242.

BRUNE, J.N. & DORMAN, J. – 1963 – Seismic waves and Earth structure in the Canadian Shield. Bull. Seismol. Soc. Am., **53**: 167-210.

BRUNE, J.N., NAFE, J.E. & OLIVER, J.E. – 1960 – A simplified method for the analysis and synthesis of dispersed wave trains. J. Geophys. Res., **65**: 287-304.

BUNGUM, H. & CAPON, J. – 1974 – Coda pattern and multipath propagation of Rayleigh waves at NORSAR. Phys. Earth Planet. Inter., **9**: 111-127.

BURKHARD, N.R. – 1977 – Upper mantle structure of the Pacific basin from inversion of gravity and seismic data. PhD thesis, University of California, Los Angeles, 169 pp.

CALCAGNILE, G., MASCIA, U., GAUDIO, V. del & PANZA, G.F. – 1984 – Deep structure of southeastern Europa from Rayleigh waves. Tectonophysics, **110**: 189-200.

CALCAGNILE, G. & PANZA, G.F. – 1978 – Crust and upper mantle structure under the Baltic Shield and Barents Sea from the dispersion of Rayleigh waves. Tectonophysics, **47**: 59-71.

CALCAGNILE, G. & PANZA, G.F. – 1979 – Central and upper mantle structure beneath the Apennines region as inferred from the study of Rayleigh waves. J. Geophys., **45**: 319-327.

CALCAGNILE, G. & PANZA, G.F. – 1980 – Upper mantle structure of the Apulian plate from Rayleigh waves. Pure and Applied Geophysics, **118**: 823-830.

CALCAGNILE, G., PANZA, G.F. & KNOPOFF, L. – 1979 – Upper-mantle structure of north-central Italy from the dispersion of Rayleigh waves. Tectonophysics, **56**: 51-63.

CAPON, J. – 1970 – Analysis of Rayleigh-wave multipath propagation at LASA. Bull. Seismol. Soc. Am., **60**: 1701-1731.

CAPUTO, M., KNOPOFF, L., MANTOVANI, E., MUELLER, S. & PANZA, G.F. – 1976 – Rayleigh waves phase velocities and upper mantle structure in the Appenines. Annali di Geofisica, **4**: 199-214.

CHANG, F. – 1979 – The structure of the upper mantle of Eurasia and tectonic interpretation from a study of Rayleigh wave dispersion. PhD thesis, University of California, Los Angeles, 209 pp.

CHANDHURY, H.M. – 1966 – Seismic surface wave dispersion and the crust across the Gangetic basin. Indian Jour. Meteorology and G, **17**: 385-394.

DE GROOT, M.H. – 1975 – Probability and statistics. Addison-Wesley, Reading.

DORMAN, J. – 1969 – Seismic surface-wave data on the upper mantle. In: The Earth's Crust and Upper Mantle. Geophysical Monograph 13, P. Hart (Ed.), Amer. Geophys. Union, Washington, D.C., 257-265.

DZIEWONSKI, A.M. & STEIM, J.M. – 1982 – Dispersion and attenuation of mantle waves through waveform inversion. Geophys. J.R. astr. Soc., **70**: 503-527.

EWING, M. & PRESS, F. – 1959 – Determination of crustal structural from phase velocity of Rayleigh waves. Part III: The United States. Bull. Geol. Soc. Am., **70**: 229-244.

FORSYTH, D.W. – 1973 – Anisotropy and the structural evolution of the oceanic upper mantle. PhD thesis, Mass. Inst. of Technol., Cambridge, 253 pp.

FORSYTH, D.W. – 1985 – The evolution of the upper mantle beneath mid-ocean ridges. Personal communication.

FOUDA, A.A. – 1973 – The upper mantle structure under the stable regions. PhD thesis, University of California, Los Angeles, 132 pp.

GABRIEL, V.G. & KUO, J.T. – 1966 – High Rayleigh wave phase velocities for the New Delhi, India-Lahore, Pakistan profile. Bull. Seismol. Soc. Am., **56**: 1137-1145.

GONCZ, J.H., HALES, A.L. & MUIRHEAD, K.J. – 1975 – Analysis to extended periods of Rayleigh and Love wave dispersion across Australia. Geophys. J.R. astr. Soc., **41**: 81-105.

GREGERSEN, S. – 1970 – Surface wave dispersion and crust structure in Greenland. Geophys. J.R. astr. Soc., **22**: 29-39.

GUMPER, F. & POMEROY, P.W. – 1970 – Seismic wave velocities and Earth structure on the African continent. Bull. Seismol. Soc. Am., **60**: 651-668.

GUPTA, H.K., NYMAN, D.C. & LANDISMAN, M. – 1977 – Shield-like upper mantle velocity structure below the Indo-gangetic Plains: inferences drawn from long-period surface wave dispersion studies. Earth Planet. Sci. Lett., **34**: 51-55.

HAGIWARA, T. – 1958 – A note on the theory of the electromagnetic seismograph. Bull. Earthq. Res. Int., **36**: 139-164.

HARKRIDER, D.G. & ANDERSON, D.L. – 1966 – Surface wave energy from point sources in plane layered Earth models. J. Geophys. Res., **71**: 2967-2980.

HILDEBRAND, F.B. – 1974 – Introduction to Numerical Analysis. Second edition, McGraw-Hill, New York.

HUANG, P.Y. – 1985 – Focal depths and mechanisms of mid-ocean ridge earthquakes from body waveform inversion. PhD thesis, Mass. Inst. of Technol., Cambridge, 301 pp.

HUANG, P.Y., SOLOMON, S.C., BERGMAN, E.A. & NABELEK, J.L. – 1986 – Focal depths and mechanisms of Mid-Atlantic ridge earthquakes from body waveform inversion. J. Geophys. Res., **91**: 579-598.

JAMES, D.E. – 1971 – Andean crustal and upper mantle structure. J. Geophys. Res., **76**: 3246-3271.

JAMES, D.E. & LINDE, A. – 1971 – A source of major error in the digital analysis of World Wilde Standard Station seismograms. Bull. Seismol. Soc. Am., **61**: 723-728.

JEMSEK, J.P., BERGMAN, E.A., NABELEK, J.L. & SOLOMON, S.C. – 1986 – Focal depths and mechanisms of large earthquakes on the Arctic mid-ocean ridge system. J. Geophys. Res., **91**: 13993-14005.

JORDAN, T.H. – 1979a – The deep structure of the continents. Scientific American, **240**: 92-107.

JORDAN, T.H. – 1979b – Structural geology of the Earth's interior. Proc. Natl. Acad. Sci., USA, **76**: 4192-4200.

JORDAN, T.H. – 1981 – Global tectonic regionalization for seismological data analysis. Bull. Seismol. Soc. Am., **71**: 1131-1141.

KAMINUMA, K. – 1964 – Crustal structure in Japan from the phase velocity of Rayleigh waves. Part 3: Rayleigh waves from the Mindanao shock of Sept. 25, 1957. Bull. Eartqh. Res. Inst., **42**: 19-38.

KAMINUMA, K. – 1966a – The crust and upper mantle structure in Japan. Part 1: Phase velocities of Love and Rayleigh waves in central Japan. Bull. Earthq. Res. Inst., **44**: 481-494.

KAMINUMA, K. – 1966b – The crust and upper mantle structure in Japan. Part 2: Crustal structure in Japan from the phase velocity of Rayleigh waves. Bull. Earthq. Res. Inst., **44**: 495-510.

KAMINUMA, K. – 1966c – The crust and upper mantle structure in Japan. Bull. Earthq. Res. Inst., **44**: 511-518.

KAMINUMA, K. & AKI, K. – 1963 – Crustal structure in Japan from the phase velocity of Rayleigh waves. Part 2: Rayleigh waves from the Aleutian shock of March 9, 1957. Bull. Earthq. Res. Inst., **41**: 217-241.

KNOPOFF, L. – 1972 – Observation and inversion of surface-wave dispersion. Tectonophysics, **13**: 497-519.

KNOPOFF, L. – 1983 – The thickness of the lithosphere from the dispersion of surface waves. Geophys. J.R. astr. Soc., **74**: 55-81.

KNOPOFF, L., BERRY, M.J. & SCHWAB, F.A. – 1967 – Tripartite phase velocity observations in laterally heterogeneous regions. J. Geophys. Res., **72**: 2595-2601.

KNOPOFF, L., MUELER, S. & PILANT, W.L. – 1966 – Structure of the crust and upper mantle in the Alps from the phase velocity of Rayleigh waves. Bull. Seismol. Soc. Am., **56**: 1009-1044.

KNOPOFF, L. & SCHLUE, J.W. – 1972 – Rayleigh wave phase velocities for the path Addis Ababa-Nairobi. Tectonophysics, **15**: 157-163.

KNOPOFF, L., SCHLUE, J.W. & SCHWAB, F.A. – 1970 – Phase velocities of Rayleigh waves across the East Pacific Rise. Tectonophysics, **10**: 321-334.

KNOPOFF, L. & VANE, G. – 1978 – Age of East Antarctica from surface wave dispersion. Pure and Applied Geophysics, **117**: 806-815.

KOVACH, R.L. – 1978 – Seismic surface waves and crustal and upper mantle structure. Rev. Geophys. Space Phy., **16**: 1-13.

KUO, J., BRUNE, J.N. & MAJOR, M. – 1962 – Rayleigh wave dispersion in the Pacific Ocean for the period range 20 to 140 seconds. Bull. Seismol. Soc. Am., **52**: 333-357.

LANDISMAN, M., DZIEWONSKI, A.M. & SATO, Y. – 1969 – Recent improvements in the analysis of surface wave observations. Geophys. J.R. astr. Soc., **17**: 369-403.

LASS, H. & GOTTLIEB, P. – 1971 – Probability and statistics. Addison-Wesley, Reading.

LEEDS, A.R. – 1975 – Lithospheric thickness in the western Pacific. Phys. Earth Planet. Inter., **11**: 61-64.

LEVEQUE, J.J. – 1980 – Regional upper mantle S-velocity models from phase velocities of great-circle Rayleigh waves. Geophys. J.R. astr. Soc., **63**: 23-43.

LEVSHIN, A.L., SABITOVA, T.M. & VALUS, V.P. – 1966 – Joint interpretation of body and surface waves data for a district in Middle Asia. Geophys. J.R. astr. Soc., **11**: 57-66.

LIAO, A.H. – 1981 – Anisotropy in the upper mantle of Eurasia. PhD thesis, University of California, Los Angeles, 177 pp.

LYON-CAEN, H. – 1980 – Rayleigh waves phase velocities curves for paths across Europe and Africa. Unpublished manuscript.

McGARR, A. – 1969a – Amplitude variations of Rayleigh waves-propagation across a continental margin. Bull.

Seismol. Soc. Am., **59**: 1281-1305.

McGARR, A. – 1969b – Amplitude variations of Rayleigh waves: horizontal refraction. Bull. Seismol. Soc. Am., **59**: 1307-1334.

McGARR, A. – 1972 – Comments on some papers concerning amplitudes of seismic surface waves. J. Geophys. Res., **77**: 3823-3826.

MENDIGUREN, J.A. – 1971 – Focal mechanism of a shock in the middle of the Nazca plate. J. Geophys. Res., **76**: 3861-3879.

MITCHEL, R.G. – 1977 – The structure of the upper mantle of western North America from multimode Rayleigh wave dispersion. PhD thesis, University of California, Los Angeles, 177 pp.

MITROVAS, W. – 1977 – Global and regional phase velocities of long-period fundamental mode Rayleigh waves. J. Geophys., **43**: 287-298.

MOAZAMI-GOUDARZI, K. – 1974 – La vitesse de phase des ondes de Rayleigh et les structures de la croute et du manteau superieur entre Machhad et Chiraz (Iran). Pure and Applied Geophysics, **112**: 675-681.

MUELLER, S. & SPRECHER, C. – 1978 – Upper mantle structure along a profile through the eastern Alps from Rayleigh wave dispersion. In: Alps, Apennines, Hellenides. H. Closs (ed.), Intern. Geodyn. Comm., sci. report, 40-44.

NABELEK, J.L. – 1984 – Determination of earthquake source parameters from inversion of body waves. PhD thesis, Mass. Inst. of Technol., Cambridge, 361 pp.

ROMANOWICZ, B.A. – 1981 – Depth resolution of earthquakes in central Asia by moment tensor inversion of long-period Rayleigh waves: effects of phase velocity variations across Eurasia and their calibration. J. Geophys. Res., **86**: 5963-5984.

ROMANOWICZ, B.A. – 1982a – Moment tensor inversion of long period Rayleigh waves: a new approach. J. Geophys. Res., **87**: 5394-5407.

ROMANOWICZ, B.A. – 1982b – Constrainsts on the structure of the Tibet plateau from pure path phase velocities of Love and Rayleigh waves. J. Geophys. Res., **87**: 6865-6883.

ROSA, J.W.C. – 1986 – A global study on phase velocity, group velocity and attenuation of Rayleigh waves in the period range 20 to 100 seconds. PhD thesis, Mass. Inst. of Technol., Cambridge.

SAITO, M. – 1967 – Excitation of free oscillations and surface waves by a point source in a vertically heterogeneous Earth. J. Geophys. Res., **72**: 3689-3699.

SAVARENSKI, E.F., BOZHKO, G.N., KUKTIKOVA, T.I., PESHKOV, A.B., POPOY, I.I., SCHECHKOV, B.N., YURKEVICH, O.I. & YUDAKOVA, L.M. – 1969 – On the Earth structure in some regions of the USSR from surface waves data. Pure and Applied Geophysics, **73**: 99-119.

SHUDOFSKY, G.N. – 1984 – Source mechanisms and focal depths of east African earthquakes and Rayleigh wave phase velocities in Africa. PhD thesis, Princeton University, Princeton, 178 pp.

SILVER, P.G. & JORDAN, T.H. – 1981 – Fundamental spheroidal mode observations of aspherical heterogeneity. Geophys. J.R. astr. Soc., **64**: 605-634.

SOBEL, P.A. & SEGGERN, D.H. von – 1978 – Applications of surface-wave ray tracing. Bull. Seismol. Soc. Am., **68**: 1359-1380.

SORIAU, A. – 1979 – Upper mantle beneath the Paris basin and Benelux including possible volcanic anomalies in Belgium. Tectonophysics, **57**: 167-188.

SORIAU, A. & SORIAU, M. – 1983 – Test of tectonic models by great circle Rayleigh waves. Geophys. J.R. astr. Soc., **73**: 533-551.

SORIAU, A. & VADELL, M. – 1980 – The crust and upper mantle beneath the Pyrenees, from surface waves: tectonic implications. Ann. Geophys., **36**: 159-166.

SORIAU-THEVENARD, A. – 1976 – Structure of the crust and the upper mantle in the southwest of France, from surface waves. Ann. Geophys., **32**: 63-69.

STUART, G.W. – 1978 – The upper mantle structure of the North Sea region from Rayleigh wave dispersion. Geophys. J.R. astr. Soc., **52**: 367-382.

SUAREZ, G. – 1982 – Seismicity, tectonics, and surface wave propagation in the Central Andes. PhD thesis, Mass. Inst. of Technol., Cambridge, 260 pp.

NATAF, H.C., NAKANISHI, I. & ANDERSON, D.L. – 1986 – Measurements of mantle wave velocities and inversion for lateral heterogeneities and anisotropy. 3. Inversion. J. Geophys. Res., **91**: 7261-7308.

NOPONEN, I. – 1966 – Surface wave phase velocities in Finland. Bull. Seismol. Soc. Am., **56**: 1093-1104.

OKAL, E. & TALANDIER, J. – 1980 – Rayleigh-wave phase velocities in French Polynesia. Geophys. J.R. astr. Soc., **63**: 719-733.

OKAL, E.A. – 1977 – The effect of intrinsic oceanic upper-mantle heterogeneity on regionalization of long-period Rayleigh-wave phase velocities. Geophys. J.R. astr. Soc., **49**: 357-370.

OLIVER, J. – 1962 – A summary of observed seismic surface wave dispersion. Bull. Seismol. Soc. Am., **52**: 81-86.

PANZA, G.F. & CALCAGNILE, G. – 1974 – Crustal structure along the coast of California from Rayleigh waves. Phys. Earth Planet. Inter., **9**: 137-140.

PANZA, G.F., NEUNHOFER, H. & CALCAGNILE, G. – 1978 – Contribution to phase velocity investigations of Rayleigh-waves in Middle Europe. Pure and Applied Geophysics, **116**: 1299-1306.

PAPAZACHOS, B.C. – 1964 – Dispersion of Rayleigh waves in the Gulf of Mexico and Carabbean Sea. Bull. Seismol. Soc. Am., **54**: 909-925.

PAPAZACHOS, B.C. – 1969 – Phase velocities of Rayleigh waves in southeastern Europe and eastern Mediterranean Sea. Pure and Applied Geophysics, **75**: 47-55.

PATTON, H.J. – 1973 – Rayleigh wave phase velocities in the Indian ocean. Unpublished manuscript.

PATTON, H.J. – 1978 – Source and propagation effects of Rayleigh waves from central Asian earthquakes. PhD thesis, Mass. Inst. of Tech., Cambridge, 342 pp.

PATTON, H.J. – 1980 – Crust and upper mantle structure of the Eurasian continent from the phase velocity and Q of surface waves. Rev. Geophys. Space Phy., **18**: 605-625.

PAYO, G. – 1969 – Crustal structure of the Mediterranean Sea. Part II: Phase velocity and travel times. Bull. Seismol. Soc. Am., **59**: 23-42.

PAYO, G. – 1970 – Structure of the crust and upper mantle in the Iberian Shield by means of a long period triangular array. Geophys. J.R. astr. Soc., **20**: 493-508.

PAYO, G. & RUIZ de la PARTE, E. – 1974 – Dispersion of surface waves in the Iberian Peninsula and the adjacent Atlantic and Mediterranean areas. Geofisica Internac., **14**: 89-102.

PRESS, F. – 1956a – Crustal structure determined by the phase velocity method. EOS, Trans. Am. Geophys. Un., **37**: 356.

PRESS, F. – 1956b – Determination of crustal structure from phase velocity of Rayleigh waves. Part I: Southern California. Bull. Geol. Soc. Am., **67**: 1647-1658.

PROSKURYAKOVA, T.A., OVCHNNIKOVA, I.B. & VORONINA, E.B. – 1970 – The Earth's structure in the region of Crimea according to the Rayleigh waves observations. Pure and Applied Geophysics, **82**: 98-107.

PUJOL, J.B. – 1982 – Rayleigh waves spectral studies of some Alaskan intraplate earthquakes. M.S. thesis, University of Alaska, Fairbanks, 78 pp.

THOMAS, L. – 1969 – Rayleigh wave dispersion in Australia. Bull. Seismol. Soc. Am., **59**: 167-182.

THOMSON, A.A. & EVISON, F.F. – 1962: Thickness of the Earth's crust in New Zealand. N.Z.J. Geol. Geophys., **5**: 29-45.

TREHU, A.M., NABELEK, J.L. & SOLOMON, S.C. – 1981 – Source characterization of two Reykjanes Ridge earthquakes: surface waves and moment tensors; P waveform and nonorthogonal nodal planes. J. Geophys. Res., **86**: 1701-1724.

TSAI, Y.B. – 1969 – Determination of focal depths of earthquakes in mid-oceanic ridges from amplitude spectra of surface waves. PhD thesis, Mass. Inst. of Technol., Cambridge, 144 pp.

TUBMAN, K.M. – 1980 – Structure and seismic properties of Iran and the Arabian Peninsula: effects of continental collision. Unpublished manuscript.

WEIDNER, D.J. – 1972 – Rayleigh waves from mid-ocean ridge earthquakes: source and path effects. PhD thesis, Mass. Inst. of Technol., Cambridge, 256 pp.

WEIDNER, D.J. – 1974 – Rayleigh wave phase velocities in the Atlantic Ocean. Geophys. J.R. astr. Soc., **36**: 105-139.

WIGGINS, R.A. – 1976 – Interpolation of digitized waves. Bull. Seismol. Soc. Am., **66**: 2077-2081.

YOMOGIDA, K. – 1985 – Amplitude and phase variations of surface waves in a laterally heterogeneous Earth: ray- and beam-theoretical approach. PhD thesis, Mass. Inst. of Technol., Cambridge, 229 pp.

Versão recebida em: 20/04/90
Versão revista e aceita em: 06/09/90
Editor Associado: M.S. Assumpção